Synthesis of New Polydentate Nitrogen Ligands and Their Use in Ethylene Polymerization in Conjunction with Iron(II) and Cobalt(II) Bis-halides and Methylaluminoxane

Pierluigi Barbaro,[†] Claudio Bianchini,*[,†] Giuliano Giambastiani,[†] Itzel Guerrero Rios,[†] Andrea Meli,[†] Werner Oberhauser,[†] Anna M. Segarra,[†] Lorenzo Sorace,[‡] and Alessandro Toti[†]

Istituto di Chimica dei Composti Organometallici (ICCOM-CNR), Via Madonna del Piano 10, 50019 Sesto Fiorentino (Firenze), Italy, and Dipartimento di Chimica and UdR INSTM, Università di Firenze, Via della Lastruccia 3, 50019 Sesto Fiorentino (Firenze), Italy

Received May 22, 2007

Original synthetic routes to polydentate nitrogen ligands combining in the same molecular structure either 2,6-bis(imino)pyridine and (imino)pyridine moieties or two 2,6-bis(imino)pyridine units are described. The tris-imino-bis-pyridine ligands ($^{Me}\mathbf{N_5}$ and $^{iPr}\mathbf{N_5}$) and the tetrakis-imino-bis-pyridine ligand ($^{iPr}\mathbf{N_6}$) react with $FeCl_2$ and/or CoX_2 (X = Cl, Br) to give paramagnetic monometallic, homobimetallic, or heterobimetallic complexes. These have been characterized, both in the solid state and in solution, by a variety of techniques, including single-crystal X-ray diffraction analyses, magnetic susceptibility determinations, IR, vis−NIR, ^{1}H NMR, and X-band EPR spectroscopies. The combination of these analytical tools has allowed us to unravel the geometrical and electronic structure of quite complicated systems. Selected mono- and binuclear Fe^{II} and Co^{II} complexes have been used as catalyst precursors in toluene for the polymerization of ethylene to high-density polyethylene (HDPE) upon activation with MAO. From fairly good to very good catalytic activities (up to 64.5 tons of PE (mol of M)$^{-1}$ h^{-1}) have been observed. Of particular relevance is the dicobalt complex $^{iPr}\mathbf{N_6Co_2Cl_4}$, which is more active than any other known Co^{II} catalyst for the polymerization of ethylene to HDPE.

Introduction

Remarkable advances in homogeneous catalysis have been recently achieved with systems comprising late transition metals and 2,6-bis(imino)pyridine ligands. Successful reactions span from the epoxidation[1] and cyclopropanation[2] of olefins, to the enantioselective reduction of prochiral ketones,[3] to the hydrogenation of olefins,[4] to the dimerization of α-olefins,[5] to the oligomerization and polymerization of ethylene[6,7] and propene.[5,8] The most relevant and studied application is certainly the oligomerization and polymerization of ethylene, independently discovered by Brookhart, Bennett, and Gibson in 1998.[6,7] Since then, five-coordinate 2,6-bis(arylimino)pyridine Fe^{II} and Co^{II} dihalides, activated by MAO, are currently used as catalyst precursors to convert ethylene either to high-density polyethylene (HDPE) or to α-olefins with turnover frequencies (TOFs) as high as several million moles of C_2H_4 converted (mol of metal)$^{-1}$ h^{-1} (Scheme 1a).[9,10]

The advantages of 2,6-bis(arylimino)pyridine Fe^{II} and Co^{II} catalysts over other types of single-site Ziegler−Natta catalysts for ethylene homopolymerization (e.g., metallocenes, constrained geometry early transition metal complexes) are manifold, spanning from the ease of preparation and handling to the use of low-cost metals with negligible environmental impact.[9] Another intriguing feature of bis(imino)pyridine Fe^{II} and Co^{II} precursors is provided by the facile tuning of their polymerization activity by simple modifications of the ligand architecture that can be adjusted so as to allow for the use of the corresponding catalysts in heterogeneous polymerization reactions.[10] It has been shown that the number, size, nature, and regiochemistry of the substituents in the arylimino groups are of crucial importance in controlling the polymerization activity.[9,10] Moreover, due to the good compatibility with various early and late metal copolymerization catalysts, 2,6-bis(arylimino)pyridine Fe^{II} and Co^{II} dihalides can be used as oligomer-

* To whom correspondence should be addressed. E-mail: claudio.bianchini@iccom.cnr.it.

† ICCOM-CNR.

‡ Università di Firenze and UdR INSTM-Firenze.

(1) Çetinkaya, B.; Çetinkaya, E.; Brookhart, M.; White, P. S. *J. Mol. Catal. A* **1999**, *142*, 101.

(2) Bianchini, C.; Lee H. M. *Organometallics* **2000**, *19*, 1833.

(3) De Matrin, S.; Zassinovich, G.; Mestroni, G. *Inorg. Chim. Acta* **1990**, *174*, 9.

(4) Knijnenburg, Q.; Horton, A. D.; van der Heijden, H.; Kooistra, T. M.; Hettershield, D. G. H.; Smits, J. M. M.; de Bruin, B.; Budzelaar, P. H. M.; Gal, A. W. *Eur. J. Inorg. Chem.* **2004**, 1204.

(5) (a) Tellmann, K. P.; Gibson, V. C.; White, A. J. P.; Williams, D. J. *Organometallics* **2005**, *24*, 280. (b) Small, B. L.; Schmidt, R. *Chem.−Eur. J.* **2004**, *10*, 1014. (c) Small, B. L. *Organometallics* **2003**, *22*, 3178. (d) Small, B. L.; Marcucci, A. J. *Organometallics* **2001**, *20*, 5738.

(6) (a) Small, B. L.; Brookhart, M. *J. Am. Chem. Soc.* **1998**, *120*, 7143. (b) Britovsek, G. J. P.; Bruce, M.; Gibson, V. C.; Kimberley, B. S.; Maddox, P. J.; McTavish, S. J.; Solan, G. A.; White, A. J. P.; Williams, D. J. *Chem. Commun.* **1998**, 849. (c) Britovsek, G. J. P.; Mastroianni, S.; Solan, G. A.; Baugh, S. P. D.; Redshaw, C.; Gibson, V. C.; White, A. J. P.; Williams, D. J.; Elsegood, M. R. J. *Chem.−Eur. J.* **2000**, *6*, 2221.

(7) (a) Britovsek, G. J. P.; Bruce, M.; Gibson, V. C.; Kimberley, B. S.; Maddox, P. J.; Mastroianni, S.; McTavish, S. J.; Redshaw, C.; Solan, G. A.; Strömberg, S.; White, A. J. P.; Williams, D. J. *J. Am. Chem. Soc.* **1999**, *121*, 8728. (b) Small, B. L.; Brookhart, M.; Bennett, A. M. A. *J. Am. Chem. Soc.* **1998**, *120*, 4049. (c) Bennett, A. M. A. (DuPont) WO 98/27124, 1998.

(8) Small, B. L.; Brookhart, M. *Macromolecules* **1999**, *32*, 2120.

(9) (a) Britovsek, G. J. P.; Gibson, V. C.; Wass D. F. *Angew. Chem., Int. Ed.* **1999**, *38*, 428. (b) Ittel, S. D.; Johnson, L. K.; Brookhart, M. *Chem. Rev.* **2000**, *100*, 1169.

(10) (a) Bianchini, C.; Giambastiani, G.; Guerrero Rios, I.; Mantovani, G.; Meli, A.; Segarra, A. M. *Coord. Chem. Rev.* **2006**, *250*, 1391. (b) Gibson, V. C.; Redshaw, C.; Solan, G. A. *Chem. Rev.* **2007**, *107*, 1745.

10.1021/om7005062 CCC: $37.00
Publication on Web 08/01/2007

Scheme 1

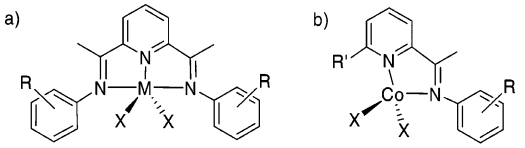

ization catalysts in tandem catalytic systems for the production of branched PE as well as in reactor blending processes to give PE with controlled molecular weight distribution and rheology.[10] The one-pot transformation of ethylene into mixtures of HDPE and α-olefins with a Schulz−Flory distribution has also been achieved with C_1-symmetric 2,6-bis(imino)pyridine Fe^{II} dihalides.[11]

The success of 2,6-bis(imino)pyridine ligands in ethylene polymerization/oligomerization has also stimulated much research aimed at developing late transition metal catalysts with (imino)pyridine ligands. A number of (mono-imino)pyridine Co^{II} catalysts are already available for the oligomerization of ethylene to α-olefins with TOFs as high as 1.5×10^6 mol of C_2H_4 converted (mol of metal)$^{-1}$ h^{-1} as well as the production of low-density polyethylene (LDPE) via tandem catalysis in conjunction with metallocenes (Scheme 1b).[12,13]

In light of the increasing number of publications and patents, the search for new molecular architectures of either 2,6-bis(imino)pyridine or (imino)pyridine ligands seems to be endless,[14] yet no example of ligands combining both structural motifs has been reported so far. Likewise, the condensation of two 2,6-bis(imino)pyridine units into a single molecule has never been described as such, the only examples of dimerization of 2,6-bis(imino)pyridine ligands being those reported by Gambarotta[15] (Scheme 2a) and by Gibson[14d] (Scheme 2b).

In this paper, we report two original synthetic routes to ligands that combine in the same molecular structure either 2,6-bis(imino)pyridine and (imino)pyridine moieties or two 2,6-bis(imino)pyridine units (Scheme 3).

We describe also the synthesis and characterization of several Fe^{II}, Co^{II}, and Ni^{II} monometallic and homo- and heterobimetallic complexes with these new polydentate nitrogen ligands, and finally, we provide some preliminary data on their use, in combination with MAO, as catalysts for the polymerization of ethylene to HDPE.

Experimental Section

General Considerations. All manipulations and reactions were carried out under an atmosphere of nitrogen using standard Schlenk techniques. Anhydrous benzene, toluene, THF, and Et_2O were obtained by means of an MBraun solvent purification system, while CH_2Cl_2 and MeOH were distilled over CaH_2 and Mg, respectively. A 10 wt % solution of methylaluminoxane (MAO) in toluene (d = 0.88 g mL^{-1}) was purchased from Aldrich. All the other reagents and solvents were used as purchased from commercial suppliers. Catalytic reactions were performed with a 500 mL stainless steel reactor, constructed at the ICCOM-CNR (Firenze, Italy), equipped with a magnetic drive stirrer and a Parr 4842 temperature and pressure controller. The reactor was connected to an ethylene reservoir to maintain a constant pressure throughout the catalytic runs. Deuterated solvents for NMR measurements were dried over 4 Å molecular sieves. ^{1}H and ^{13}C{^{1}H} NMR spectra were recorded on Bruker ACP 200 (200.13 and 50.32 MHz, respectively) and Bruker Avance DRX-400 (400.13 and 100.62 MHz, respectively) spectrometers equipped with variable-temperature control units accurate to ±0.1 °C. Chemical shifts are reported in ppm (δ) relative to TMS or referenced to the chemical shifts of residual solvent resonances (^{1}H and ^{13}C). The number of protons attached to the carbon nuclei was determined by means of both ^{13}C{^{1}H} DEPT 135 and J-modulated spin−echo NMR pulse programs. The assignment of the signals was achieved with the aid of 1D spectra, 2D ^{1}H COSY, ^{1}H NOESY, and proton detected ^{1}H−^{13}C correlations (HMQC) using nonspinning samples. 2D NMR spectra were recorded with pulse sequences suitable for phase-sensitive representations using TPPI. ^{1}H NOESY measurements[16] were recorded with 1024 increments of size 2 K (with 8 scans each) covering the full range in both dimensions and with mixing times of 800 and 300 ms. ^{1}H−^{13}C HMQC correlations[17] were recorded by use of the standard sequence with decoupling during acquisition. Elemental

Scheme 2

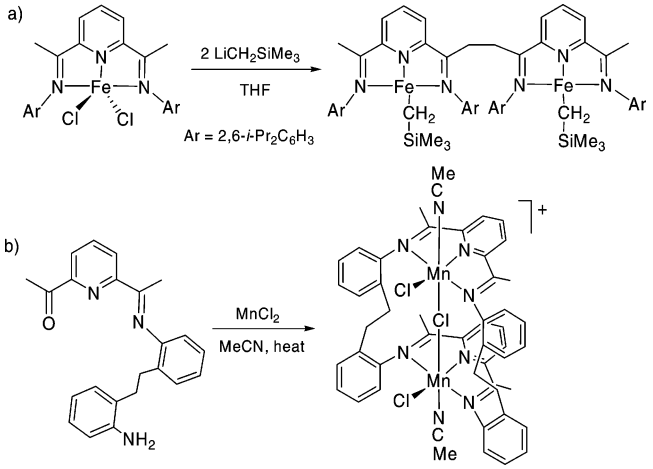

Scheme 3

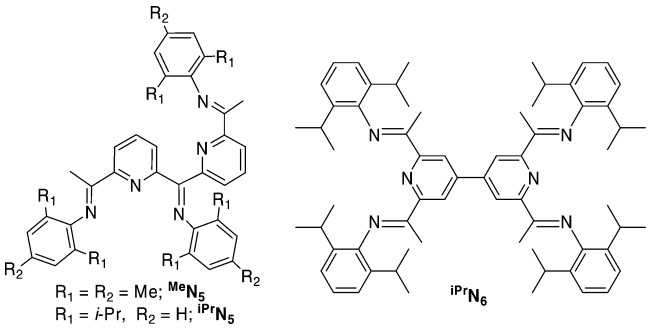

(11) Bianchini, C.; Giambastiani, G.; Guerrero Rios, I.; Meli, A.; Passaglia, E.; Gragnoli, T. *Organometallics.* **2004**, *23*, 6087.

(12) (a) Bianchini, C.; Mantovani, G.; Meli, A.; Migliacci, F.; Laschi, F. *Organometallics* **2003**, *22*, 2545. (b) Bianchini, C.; Giambastiani, G.; Mantovani, G.; Meli, A.; Mimeau, D. *J. Organomet. Chem.* **2004**, *689*, 1356. (c) Bianchini, C.; Gatteschi, D.; Giambastiani, G.; Guerrero Rios, I.; Ienco, A.; Laschi, F.; Mealli, C.; Meli, A.; Sorace, L.; Toti, A.; Vizza, F. *Organometallics.* **2007**, *26*, 726.

(13) Bianchini, C.; Frediani, M.; Giambastiani, G.; Kaminsky, W.; Meli, A.; Passaglia, E. *Macromol. Rapid Commun.* **2005**, *26*, 1218.

(14) (a) Wang, L.; Sun, W.-H.; Han, L.; Yang, H.; Hu, Y.; Jin, X. *J. Organomet. Chem.* **2002**, *658*, 62. (b) Britovsek, G. J. P.; Baugh, S. P. D.; Hoarau, O.; Gibson, V. C.; Wass D. F., White, A. J. P.; Williams, D. J. *Inorg. Chim. Acta* **2003**, *345*, 279. (c) Liu, Jingyu; Li, Y.; Liu, Jingyao; Li, Z. *Macromolecules* **2005**, *38*, 2559. (d) Gibson, V. C.; McTavish, S. J.; Redshaw, C.; Solan, G. A.; White, A. J. P.; Williams, D. J. *Dalton Trans.* **2003**, 221. (e) Champouret, Y. D. M.; Maréchal J.-D.; Dadhiwala, I.; Fawcett, J.; Palmer, D.; Singh, K.; Solan G. A. *Dalton Trans.* **2006**, 2350.

(15) Scott, J.; Gambarotta, S.; Korobkov, I.; Budzelaar, P. H. M. *J. Am. Chem. Soc.* **2005**, *127*, 13019.

(16) (a) Sklener, V.; Miyashiro, H.; Zon, G.; Miles, H. T.; Bax, A. *FEBS Lett.* **1986**, *208*, 94. (b) Jeener, J.; Meier, B. H.; Bachmann, P.; Ernst, R. R. *J. Chem. Phys.* **1979**, *71*, 4546.

(17) Bax, A. A.; Griffey, R. H.; Hawkins, B. L. *J. Magn. Reson.* **1983**, *55*, 301.

analyses were performed using a Carlo Erba model 1106 elemental analyzer with an accepted tolerance of ±0.4 unit on carbon (C), hydrogen (H), and nitrogen (N). Melting points were ensued by using a Stuart Scientific melting point apparatus SMP3. Conductivity measurement was obtained with an Orion model 990101 conductance cell connected to a model 101 conductivity meter. The conductivity data[18] were obtained at sample concentrations of ca. 10^{-3} M in 1,2-dichloroethane solution. Magnetic moments were measured at 22 °C with a Cryogenic SQUID S600 magnetometer at three different applied magnetic fields (0.5, 1, and 2 T). Raw data were corrected for the diamagnetism of the sample holder, measured in the same conditions, and for the intrinsic diamagnetism of the sample, estimated through Pascal's constants. Vis−NIR spectra (range 25000-4550 cm^{-1}) in both solid state (reflectance) and CH_2Cl_2 solution (absorption) were recorded on a Perkin-Elmer Lamda 9 spectrophotometer. Infrared spectra were recorded with a Perkin-Elmer Spectrum BX FT-IR spectrophotometer. X-band EPR spectra on both powder and frozen solution (CH_2Cl_2) samples were recorded on a Bruker Elexsys E500 spectrometer equipped with a ^{4}He continuous flow cryostat for operation at cryogenic temperature (4−20 K). GC analyses were performed with a Shimadzu GC-17 gas chromatograph equipped with a flame ionization detector and a 30 m (0.25 mm i.d., 0.25 μm film thickness) SPB-1 Supelco fused silica capillary column. GC/MS analyses were performed on a Shimadzu QP 5000 apparatus equipped with a column identical with that used for GC analysis. DSC (differential scanning calorimetry) spectroscopic analyses were obtained using a Perkin-Elmer DSC7 instrument at a heating rate of 20 °C/min from 40 to 200 °C. Calibration of both temperature and enthalpy was made with a standard sample of In and Zr. The molecular weight (M_w) and molecular weight distribution (M_w/M_n) of the polymers were evaluated by gel permeation chromatography (GPC) with a Waters GPC 2000 system equipped with a set of three columns, Styragel HT6, HT5, and HT3, and a refractive index detector. The analyses were performed at 140 °C using 1,2,4-trichlorobenzene as solvent with an elution time of 1 mL min^{-1} and standard polystyrene as the reference.

Synthesis of 1-(6-Bromopyridin-2-yl)ethanone.[19] To a stirred solution of 2,6-dibromopyridine (7.11 g, 30.0 mmol) in Et_2O (130 mL) at −78 °C was added a 1.7 M solution of *t*-BuLi in *n*-pentane (18.8 mL, 30.0 mmol) within 10 min. After 30 min of stirring at −78 °C, *N*,*N*-dimethylacetamide (3.1 mL, 33.0 mmol) was added and stirring was maintained for a further 1.5 h. The resulting mixture was allowed to warm at room temperature and treated with water (30 mL). The formed layers were separated. The aqueous layer was extracted with Et_2O (3 × 30 mL), and the collected organic layers were washed with water (2 × 30 mL). The organic phase was dried over Na_2SO_4, and the solvent was removed under reduced pressure to give a yellow crude oil, which solidified upon cooling at −20 °C in petroleum ether. After 6 h, small, pale yellow crystals were separated by filtration (yield 90%). Mp: 44 °C. IR (KBr): ν 1695 cm^{-1}(C═O). ^{1}H NMR ($CDCl_3$): δ 2.70 (s, 3H, C(O)Me), 7.68 (m, 2H, Py-H_m/H_p), 7.98 (dd, J = 6.5, 2.1 Hz, 1H, Py-H_m). $^{13}C\{^1H\}$ NMR ($CDCl_3$): δ 26.4 (1C, C(O)*Me*), 121.1 (1C, Py-CH), 132.4 (1C, Py-CH), 139.8 (1C, Py-CH), 142.0 (1C, Py-C), 154.9 (1C, Py-C), 198.5 (1C, *C*(O)Me). Anal. Calcd (%) for C_7H_6BrNO (200.03): C, 42.03; H, 3.02; N, 7.00. Found: C, 42.09; H, 2.90; N, 7.02.

Synthesis of 6-Bromo-2-(2′-methyl-1′,3′-dioxolan-2′-yl)pyridine.[20] A solution of 1-(6-bromopyridin-2-yl)ethanone (1.0 g, 5 mmol), 1,2-ethanediol (0.34 mL, 6 mmol), and 4-toluenesulfonic acid (0.1 g, 0.5 mmol) in benzene (15 mL) was heated at reflux temperature for 24 h in a Dean−Stark apparatus. The mixture was cooled to room temperature and then treated with 5 mL of a 0.5 M aqueous NaOH solution. The formed layers were separated. The aqueous phase was washed with Et_2O (2 × 5 mL), and the combined organic extracts were dried over $NaSO_4$. After removal of the solvent under reduced pressure a white solid was obtained in a pure form (yield >99%). Mp: 40−42 °C. ^{1}H NMR ($CDCl_3$): δ 1.80 (s, 3H, Me), 3.95−4.20 (m, 4H, CH_2), 7.49 (dd, J = 7.7, 1.3 Hz, 1H, Py-H_m), 7.58−7.65 (m, 2H, Py-H_m/H_p). $^{13}C\{^1H\}$ NMR ($CDCl_3$): δ 25.6 (1C, Me), 65.6 (2C, CH_2), 108.5 (1C, OCO), 118.9 (1C, Py-CH_m), 128.1 (1C, Py-CH_m), 139.6 (1C, Py-CH_p), 142.5 (1C, Py-C-Br), 163.0 (1C, Py-C-CO). Anal. Calcd (%) for $C_9H_{10}BrNO_2$ (244.09): C, 44.29; H, 4.13; N, 5.74. Found: C, 44.09; H, 4.22; N, 5.69.

Synthesis of Bis[3-(2-methyl-[1,3]dioxolan-2-yl)pyridin-2-yl]-methanone. A solution of 6-bromo-2-(2′-methyl-1′,3′-dioxolan-2′-yl)pyridine (2.64 g, 10.81 mmol) in 50 mL of THF at −78 °C was treated dropwise with a 1.7 M solution of *t*-BuLi in *n*-pentane (6.67 mL, 11.35 mmol) over 15 min. After 30 min at −78 °C, methylchloroformate (0.42 mL, 5.40 mmol) was added dropwise over 10 min. The reaction mixture was stirred for an additional 1 h at −78 °C and then allowed to warm at room temperature overnight. Brine was added, and the phases were separated. The aqueous layer was extracted with 30 mL of Et_2O and subsequently with CH_2Cl_2 (2 × 25 mL). The combined organic layers were dried over Na_2SO_4, and after removal of solvents under reduce pressure, a pale yellow solid was obtained as the pure product (yield 91%). Mp: 96−97 °C. IR (KBr): ν 1677 cm^{-1} (C═O). ^{1}H NMR ($CDCl_3$): δ 1.73 (s, 6H, Me), 3.88−4.13 (m, 8H, CH_2), 7.73 (dd, J = 7.7, 1.3 Hz, 2H, Py-H_m), 7.88 (dd, J = 7.7, 7.6 Hz, 2H, Py-H_p), 8.03 (dd, J = 7.6, 1.3 Hz, 2H, Py-H_m) $^{13}C\{^1H\}$ NMR ($CDCl_3$): δ 25.5 (2C, Me), 65.7 (4C, CH_2), 109.2 (2C, OCO), 122.6 (2C, Py-CH), 125.0 (2C, Py-CH), 137.7 (2C, Py-CH_p), 154.9 (2C, Py-C), 160.9 (2C, Py-C), 193.7 (2C, C═O). Anal. Calcd (%) for $C_{19}H_{20}N_2O_5$ (356.38): C, 64.04; H, 5.66; N, 7.86. Found: C, 64.10; H, 5.73; N, 7.78.

Synthesis of 1-[6-(6-Acetylpyridine-2-carbonyl)pyridin-2-yl]-ethanone. Bis[3-(2-methyl-[1,3]dioxolan-2-yl)pyridin-2-yl]methanone (1.50 g, 4.21 mmol) was suspended in 2 M HCl (15 mL) and stirred at 80−85 °C for 2 h. The resulting mixture was then cooled in an ice bath, diluted with iced water (15 mL), and neutralized with solid $NaHCO_3$ portionwise. A standard extractive workup with ethyl acetate (EtOAc, 3 × 50 mL) gave, after removal of solvent, a crude, slightly brown solid, which was purified by filtration on a silica gel pad (EtOAc/petroleum ether, 95:5) to afford the expected compound as pure, pale yellow crystals (yield >99%). Mp: 97−99 °C. IR (KBr): ν 1697, 1686 cm^{-1} (C═O). ^{1}H NMR ($CDCl_3$): δ 2.61 (s, 6H, C(O)Me), 8.07 (td, J = 8.0, 7.6 Hz, 2H, Py-H_p), 8.25 (dd, J = 8.0, 1.3, Hz, 2H, Py-H_m), 8.30 (dd, J = 7.6, 1.3, Hz, 2H, Py-H_m). $^{13}C\{^1H\}$ NMR ($CDCl_3$): δ 26.2 (2C, Me), 124.8 (2C, Py-CH), 128.7 (2C, Py-CH), 138.3 (2C, Py-CH_p), 153.3 (2C, Py-C), 153.9 (2C, Py-C), 192.4 (1C, C═O), 200.1 (2C, C(O)Me). Anal. Calcd (%) for $C_{15}H_{12}N_2O_3$ (268.27): C, 67.16; H, 4.51; N, 10.44. Found: C, 67.12; H, 4.57; N, 10.37.

Synthesis of {6-[1-(2,6-Diisopropylphenylimino)ethyl]pyridin-2-yl}-{6-[1-(2,6-diisopropylphenylimino)ethyl]pyridin-3-yl}-methanone ($^{Me}N_5$). A mixture of 1-[6-(6-acetylpyridine-2-carbonyl)-pyridin-2-yl]ethanone (0.52 g, 1.94 mmol) and 2,4,6-trimethylaniline (1.8 mL, 1.73 g, 12.8 mmol) was dissolved in MeOH (20 mL) containing a few drops of formic acid, and the resulting mixture was heated to reflux of solvent for 3 days. The resulting yellow-orange solution was cooled to −24 °C. After 2 days, yellow crystals of the desired product were isolated by filtration (yield 92%). Mp: 180−181 °C. IR (KBr): ν 1643 cm^{-1} (C═N). ^{1}H NMR ($CDCl_3$): δ 1.84 (s, 3H, N═CMe), 1.93 (s, 6H, Ar−Me_o), 1.94 (s, 3H, N═CMe), 1.99 (s, 6H, Ar-Me_o), 2.09 (s, 6H, Ar-Me_o), 2.19 (s, 3H, Ar-Me_p), 2.30 (s, 3H, Ar-Me_p), 2.31 (s, 3H, Ar-Me_p), 6.71 (s, 2H, Ar-H_m), 6.88 (s, 2H, Ar-H_m), 6.90 (s, 2H, Ar-H_m), 7.54 (dd, J =

(18) Geary, W. J. *J. Coord. Chem. Rev.* **1971**, *7*, 81. (b) Morassi, R.; Sacconi, L. *J. Chem. Soc. A* **1971**, 492.

(19) Bolm, C.; Ewald, M.; Schilingloff, G. *Chem. Ber.* **1992**, *125*, 1169.

(20) Constable, E. C.; Heirtzler, F.; Neuburger, N.; Zehnder, M. *J. Am. Chem. Soc.* **1997**, *119*, 5606.

7.7, 0.8 Hz, 1H, Py-H$_m$), 7.74 (t, J = 7.9 Hz, 1H, Py-H$_p$), 8.02 (t, J = 7.8 Hz, 1H, Py-H$_p$), 8.17 (dd, J = 7.9, 0.8 Hz, 1H, Py-H$_m$), 8.51 (dd, J = 8.0, 0.9 Hz, 1H, Py-H$_m$), 8.64 (dd, J = 7.9, 0.8 Hz, 1H, Py-H$_m$). ^{13}C{^{1}H} NMR ($CDCl_3$): δ 16.50 (1C, N=C*Me*), 16.61 (1C, N=C*Me*), 18.03 (1C, Ar-*p*-Me), 18.14 (2C, Ar-Me$_o$), 18.26 (2C, Ar-Me$_o$), 18.84 (2C, Ar-Me$_o$), 21.03 (1C, Ar-Me$_p$), 21.08 (1C, Ar-Me$_p$), 122.54 (1C, Py-CH$_m$), 122.75 (1C, Py-CH$_m$), 123.44 (1C, Ar-C$_p$), 123.56 (1C, Ar-C$_p$), 123.61 (1C, Ar-C$_p$), 124.33 (1C, Py-CH$_m$), 126.13 (1C, Py-CH$_m$), 128.46 (2C, Ar-CH$_m$), 128.93 (2C, Ar-CH$_m$), 128.93 (2C, Ar-CH$_m$), 135.22 (2C, Ar-C$_o$), 135.66 (1C, Py-CH$_p$), 135.98 (2C, Ar-C$_o$), 136.13 (2C, Ar-C$_o$), 137.66 (1C, Py-CH$_p$), 146.75 (1C, Ar-C$_i$), 146.79 (1C, Ar-C$_i$), 146.82 (1C, Ar-C$_i$), 152.51 (1C, N=*C*Me), 155.42 (1C, Py-C), 155.53 (1C, Py-C), 155.71 (1C, Py-C), 155.77 (1C, Py-C), 164.48 (1C, N=*C*Me), 164.89 (1C, N=*C*Me). Anal. Calcd (%) for $C_{42}H_{45}N_5$ (619.84): C, 81.38; H, 7.32; N, 11.30. Found: C, 81.52; H, 7.26; N, 11.41.

Synthesis of {6-[1-(2,6-Diisopropylphenylimino)ethyl]pyridin-2-yl}-{6-[1-(2,6-diisopropylphenylimino)ethyl]pyridin-3-yl}-methanone (^{iPr}N$_5$). A mixture of 1-{6-[(6-acetyl-2-pyridinyl)-carbonyl]-2-pyridinyl}-1-ethanone (0.77 g, 2.87 mmol) and 2,6-diisopropylaniline (tech. 90%, 3.0 mL, 14.4 mmol) in MeOH (20 mL) containing a few drops of formic acid was heated to reflux of solvent for 72 h. The resulting yellow-orange solution was cooled to −24 °C. After 2 days, yellow crystals of the desired product were isolated by filtration (yield 84%). Mp: 194−195 °C. IR (KBr): ν 1646 cm^{-1} (C=N). ^{1}H NMR ($CDCl_3$): δ 1.00 (d, J = 6.8 Hz, 6H, CHMe*Me*), 1.13 (d, J = 7.0 Hz, 6H, CHMe*Me*), 1.14 (d, J = 7.0 Hz, 6H, CHMe*Me*), 1.18 (d, J = 6.9 Hz, 6H, CH*Me*Me), 1.22 (d, J = 6.9 Hz, 6H, CH*Me*Me), 1.25 (d, J = 6.8 Hz, 6H, CH*Me*Me), 1.79 (s, 3H, N=CMe), 2.04 (s, 3H, N=CMe), 2.66 (spt, J = 6.8 Hz, 2H, C*H*Me$_2$), 2.79 (spt, J = 6.8 Hz, 2H, C*H*Me$_2$), 3.04 (spt, J = 6.8 Hz, 2H, C*H*Me$_2$), 7.01 (m, 1H, Ar-H$_p$), 7.06 (m, 2H, Ar−H$_m$), 7.12 (m, 1H, Ar-H$_p$), 7.18 (m, 2H, Ar-H$_m$), 7.19 (m, 1H, Ar-H$_p$), 7.22 (m, 2H, Ar-H$_m$), 7.59 (d, J = 7.7 Hz, 1H, Py-H$_m$), 7.78 (t, J = 7.9 Hz, 1H, Py-H$_p$), 8.06 (t, J = 7.8 Hz, 1H, Py-H$_p$), 8.26 (d, J = 7.8 Hz, 1H, Py-H$_m$), 8.57 (d, J = 7.8 Hz, 1H, Py-H$_m$), 8.66 (d, J = 7.7 Hz, 1H, Py-H$_m$). ^{13}C{^{1}H} NMR ($CDCl_3$): δ 17.35 (1C, N=C*Me*), 17.72 (1C, N=C*Me*), 22.37 (2C, CH*Me*Me), 23.30 (2C, CH*Me*Me), 23.33 (2C, CH*Me*Me), 23.55 (2C, CHMe*Me*), 23.65 (2C, CHMe*Me*), 24.08 (2C, CHMe*Me*), 28.65 (2C, *C*HMe$_2$), 28.77 (2C, *C*HMe$_2$), 28.97 (2C, *C*HMe$_2$), 121.11 (1C, Py-CH$_m$), 122.46 (1C, Py-CH$_m$), 122.97 (2C, Ar-CH$_m$), 123.35 (2C, Ar-CH$_m$), 123.42 (2C, Ar-CH$_m$), 123.87 (1C, Ar-CH$_p$), 123.94 (1C, Ar-CH$_p$), 124.06 (1C, Ar-CH$_p$), 124.84 (1C, Py-CH$_m$), 126.90 (1C, Py-CH$_m$), 135.42 (2C, Ar-*o*-C), 136.01 (1C, Py-CH$_p$), 136.11 (2C, Ar-*o*-C), 136.18 (2C, Ar-*o*-C), 137.66 (1C, Py-CH$_p$), 146.79 (2C, Ar-*ipso*-C), 146.94 (1C, Ar-*ipso*-C), 152.45 (1C, N=*C*Me), 155.27 (1C, Py-C), 155.32 (1C, Py-C), 155.50 (1C, Py-C), 155.52 (1C, Py-C), 167.20 (1C, N=*C*Me), 167.83 (1C, N=*C*Me). Anal. Calcd (%) for $C_{51}H_{63}N_5$ (746.08): C, 82.10; H, 8.51; N, 9.39. Found: C, 82.03; H, 6.44; N, 9.48.

Synthesis of 1-(6,2′,6′-Triacetyl[4,4′]bipyridinyl-2-yl)ethanone.[21] To a suspension of 4,4′-bipyridyl (5 g, 33 mmol) in acetic acid (30 mL) cooled in an ice bath were added $FeSO_4$·$7H_2O$ (20 g), acetaldehyde (20 mL), and H_2SO_4 (1.6 mL) in sequence. The slurry was treated dropwise under vigorous stirring at 0 °C with *t*-BuOOH (20 mL, 220 mmol). Within 20 min the reaction mixture turned to an orange solution with exothermicity. After 3 h the reaction mixture was warmed to room temperature and stirred 1 h further. During this time a white precipitate was formed. The suspension was poured onto ice (200 g), and after dissolution the remaining solid was separated by filtration. A standard extractive procedure with CH_2Cl_2 (3 × 50 mL) achieved, after removal of solvent under reduced pressure, a white solid. The desired product was purified by flash chromatography (CH_2Cl_2/*n*-pentane/EtOAc, 70:25:5), providing a white solid (yield 12%). Mp: 262 °C. IR (KBr): ν 1705 cm^{-1} (C=O). ^{1}H NMR ($CDCl_3$): δ 2.85 (s, 12H, C(O)Me), 8.56 (s, 4H, Py-H$_m$). Anal. Calcd (%) for $C_{18}H_{26}N_2O_4$ (324.33): C, 66.66; H, 4.97; N, 8.64. Found: C, 66.51; H, 4.92; N, 8.55.

Synthesis of 2,6,2′,6′-(2,6-Diisopropylphenyl)ethylideneamine-[4,4′]bipyridinyl (^{iPr}N$_6$). A suspension of 1-(6,2′,6′-triacetyl[4,4′]-bipyridinyl-2-yl)ethanone (300 mg, 0.925 mmol) in *n*-BuOH (6 mL) was treated with 2,6-diisopropylaniline (2.62 mL, 13.87 mmol) and a catalytic amount of formic acid (0.06 mL, 1.6 mmol), then refluxed for 20 h. After that time, the reaction mixture was cooled at 4 °C overnight and a yellow solid separated. The resulting pure, yellow crystalline product was filtered and washed several times with cold MeOH (yield 91%). IR (KBr): ν 1646 cm^{-1} (C=N). ^{1}H NMR (CD_2Cl_2): δ 1.16 (d, J = 6.8, 24H, CHMe*Me*), 1.20 (d, J = 6.9, 24H, CH*Me*Me), 2.34 (s, 12H, N=CMe), 2.82 (sept, J = 6.8, 8H, C*H*Me$_2$), 7.12 (t, J = 7.4, 4H, Ar-H$_p$), 7.21 (d, J = 7.4, 8H, Ar-H$_m$), 8.85 (s, 4H, Py-H$_m$). ^{13}C{^{1}H} NMR (CD_2Cl_2): δ 17.00 (4C, N=C*Me*), 22.5 (8C, CH*Me*Me), 23.08 (8C, CHMe*Me*), 28.30 (8C, *C*HMe$_2$), 120.58 (4C, Py-CH$_m$), 122.95 (8C, Ar-CH$_m$), 123.62 (4C, Ar-CH$_p$), 135.75 (8C, Ar-C$_o$), 146.36 (4C, Ar-C$_i$), 147.63 (2C, Py-C$_p$), 156.10 (4C, Py-C$_o$), 166.78 (4C, N*C*Me). Anal. Calcd (%) for $C_{66}H_{84}N_6$ (961.43): C, 82.45; H, 8.81; N, 8.74. Found: C, 82.37; H, 8.76; N, 8.81.

Synthesis of ^{Me}N$_5$FeCl$_2$. A suspension of $FeCl_2$ (16 mg, 0.124 mmol) in THF (4 mL) was added dropwise to a yellow solution of ^{Me}N$_5$ (77 mg, 0.124 mmol) in diethyl ether (Et_2O, 20 mL) at room temperature. The resulting dark solution was maintained under stirring for 12 h at room temperature. During this time the product precipitated as a green powder. Further precipitation was obtained by concentration to small volume under a stream of nitrogen and addition of Et_2O (20 mL). The complex was isolated by decantation, washed with a 1:1 mixture of Et_2O/*n*-pentane, and dried under vacuum (yield 90%). IR (KBr): ν 1641, 1617 cm^{-1} (C=N). μ_{eff}: 5.36 μ_B (22 °C). Electronic spectra: (reflectance) 13 800, 4900sh cm^{-1}; (absorption) 14 000 (ϵ 1000), 4900 (ϵ 25) cm^{-1}. Anal. Calcd (%) for $C_{42}H_{45}Cl_2FeN_5$ (746.61): C, 67.57; H, 6.08; Fe, 7.48; N, 9.38. Found: C, 67.60; H, 6.12; Fe, 7.50; N, 9.33.

Synthesis of ^{Me}N$_5$Fe$_2$Cl$_4$. A suspension of $FeCl_2$ (31 mg, 0.248 mmol) in THF (4 mL) was added to a stirred solution of ^{Me}N$_5$ (77 mg, 0.124 mmol) in CH_2Cl_2 (10 mL) at room temperature. Standing overnight the resulting dark solution produced the product as dark brown powder. The complex was isolated by decantation, washed with *n*-pentane, and dried under vacuum (yield 70%). IR (KBr): ν 1617 cm^{-1} (C=N). μ_{eff}: 7.04 μ_B (22 °C). Electronic spectra: (reflectance) 13 800, 4900 cm^{-1}. Anal. Calcd (%) for $C_{42}H_{45}Cl_4Fe_2N_5$ (873.36): C, 57.76; H, 5.19; Fe, 12.79; N, 8.02. Found: C, 57.74; H, 5.21; Fe, 12.80; N, 8.00.

Synthesis of ^{iPr}N$_5$CoCl$_2$. Dropwise addition of $CoCl_2$ (16 mg, 0.124 mmol) in THF (3 mL) to ^{iPr}N$_5$ (92 mg, 0.124 mmol) in Et_2O (30 mL) at room temperature yielded a dark brown solution. After 10 min the precipitation of a small crop of the product as a brown solid occurred. The mixture was allowed to stand overnight under stirring. The product was collected by decantation, washed with small portions of Et_2O and *n*-pentane, and dried under vacuum (yield 84%). IR (KBr): ν 1648, 1615 cm^{-1} (C=N). μ_{eff}: 4.55 μ_B (22 °C). Electronic spectra: (reflectance) 17 850sh, 15 050, 11 800, 8350, 6700 cm^{-1}; (absorption) 17 900sh, 14 600 (ϵ 102), 11 800 (ϵ 10), 8350 (ϵ 15), 6900 (ϵ 25) cm^{-1}. Anal. Calcd (%) for $C_{51}H_{63}Cl_2CoN_5$ (875.93): C, 69.93; H, 7.25; N, 8.00. Found: C, 69.90; H, 7.28; N, 7.95.

Synthesis of ^{Me}N$_5$CoCl$_2$. Employing an analogous procedure to that described above, but using the ligand ^{Me}N$_5$ (77 mg, 0.124 mmol), gave ^{Me}N$_5$CoCl$_2$ as a brown solid in 82% yield. IR (KBr): ν 1642, 1617 cm^{-1} (C=N). μ_{eff}: 4.68 μ_B (22 °C). Electronic spectra: (reflectance) 18 200sh, 15 000, 11 500, 8300, 7050 cm^{-1}; (absorption) 18 300sh, 14 650 (ϵ 110), 11 600 (ϵ 8), 8300 (ϵ 18), 6900 (ϵ 30) cm^{-1}. ^{1}H NMR (CD_2Cl_2, all peaks appear as broad

(21) Citterio, A.; Arnoldi, A.; Macrì, C. *Chim. Ind.* **1978**, *60*, 14.

singlets): six-coordinate species δ 62.64 (1H), 60.59 (1H), 17.44 (6H), 14.28 (6H), 11.31 (3H), 10.92 (3H), 8.21 (3H), 7.68 (1H), 6.9 (2+1H), 2.41 (3H), 2.05 (2+1H), 1.95 (2H), −2.98 (3H), −3.38 (6H), −8.95 (1H). Anal. Calcd (%) for $C_{42}H_{45}Cl_2CoN_5$ (749.69): C, 67.36; H, 6.06; Co, 7.88; N, 9.36. Found: C, 65.95; H, 5.93; Co, 6.65; N, 10.45.

Synthesis of $^{Me}N_5CoBr_2$. Employing an analogous procedure to that described above, but using $CoBr_2$ (27 mg, 0.124 mmol), gave the product as a orange solid in 80% yield. IR (KBr): ν 1617 cm^{-1} (C═N); (CH_2Cl_2): ν 1642, 1617 cm^{-1} (C═N). μ_{eff}: 4.74 μ_B (22 °C). Electronic spectra: (reflectance) 17 800sh, 9900 cm^{-1}; (absorption) 17 900sh, 14 600 (ϵ 90), 10 500 (ϵ 24), 8200 (ϵ 21), 6900 (ϵ 28) cm^{-1}. ^1H NMR (CD_2Cl_2, all peaks appear as broad singlets): 114.10 (1H), 111.95 (1H), 70.15 (1H), 66.01 (1H), 49.85 (1H), 43.90 (1H), 43.75 (1H), 28.85 (6H), 23.45 (6H), 22.21 (3H), 19.96 (3H), 15.80 (3H), 14.04 (3H), 12.11 (3H), 9.45 (1H), 9.21 (2H), 8.89 (1H), 6.99 (2H), 6.48 (2H), 6.11 (1H), 3.45 (3H), 2.11 (2H), 1.9 (3+3+2H), 1.5 (2+1H), 1.18 (6H), 0.8 (3+3H), 0.28 (6H), −1.38 (1H), −23.21 (6H), −25.85 (6H). Anal. Calcd (%) for $C_{42}H_{45}Br_2CoN_5$ (838.59): C, 60.28; H, 5.42; Co, 7.05; N, 8.37. Found: C, 60.40; H, 5.80; Co, 6.93; N, 8.21.

Synthesis of $^{Me}N_5Co_2Cl_4$. Dropwise addition of a solution of $^{Me}N_5$ (77 mg, 0.124 mmol) in THF (2 mL) to a stirred solution of $CoCl_2$ (32 mg, 0.248 mmol) in THF (6 mL) at 60 °C yielded a green solution. After 7 h, the solution was cooled to room temperature, and the green solid was collected by decantation, washed with small portions of Et_2O and *n*-pentane, and dried under vacuum (yield 82%). IR (KBr): ν 1617 cm^{-1} (C═N). μ_{eff}: 6.36 μ_B (22 °C). Electronic spectra: (reflectance) 17 250, 15 000, 11 300, 9050, 8200, 7000 cm^{-1}. Anal. Calcd (%) for $C_{42}H_{45}Cl_4Co_2N_5$ (879.53): C, 57.36; H, 5.16; Co, 13.40; N, 7.96. Found: C, 57.40; H, 5.19; Co, 13.43; N, 7.88.

Synthesis of $^{Me}N_5Co_2Br_4$. A solution of $CoBr_2$ (14 mg, 0.062 mmol) in THF (2 mL) was added to a stirred suspension of $^{Me}N_5CoBr_2$ (52 mg, 0.062) in THF (2 mL) at room temperature. A green solution immediately formed, from which a small amount of a green solid separated after a few minutes. After 8 h, the product was collected by decantation, washed with small portions of Et_2O and *n*-pentane, and dried under vacuum (yield 90%). IR (KBr): ν 1617 cm^{-1} (C═N). μ_{eff}: 6.42 μ_B (22 °C). Electronic spectra: (reflectance) 16 400, 14 450, 11 100, 8950, 8400, 6600 cm^{-1}. Anal. Calcd (%) for $C_{42}H_{45}Br_4Co_2N_5$ (1057.34): C, 47.71; H, 4.29; Co, 11.15; N, 6.62. Found: C, 47.69; H, 4.27; Co, 11.12; N, 6.64.

$^{Me}N_5CoFeCl_4$. A suspension of $FeCl_2$ (8 mg, 0.062 mmol) in THF (4 mL) was added to a solution of $^{Me}N_5CoCl_2$ (46 mg, 0.062) in CH_2Cl_2 (20 mL) at room temperature to yield immediately a dark solution, which was stirred for 24 h. The formed green-brown product was collected by decantation, washed with small portions of Et_2O and *n*-pentane, and dried under vacuum (yield 90%). IR (KBr): ν 1620 cm^{-1} (C═N). μ_{eff}: 6.82 μ_B (22 °C). Electronic spectra: (reflectance) 18 200sh, 15 000, 11 000, 8250, 7000 cm^{-1}. Anal. Calcd (%) for $C_{42}H_{45}Cl_4CoFeN_5$ (876.44): C, 57.56; H, 5.18; Co, 6.72; Fe, 6.37; N, 7.99. Found: C, 57.41; H, 5.14; Co, 6.65; Fe, 6.28; N, 7.97.

$^{Me}N_5CoNiBr_2Cl_2$. A suspension of $NiBr_2 \cdot MeOCH_2CH_2OMe$ (19 mg, 0.062 mmol) in THF (3 mL) was added to a solution of $^{Me}N_5CoCl_2$ (46 mg, 0.062) in CH_2Cl_2 (20 mL) at room temperature. After 24 h, the formed light green product was collected by decantation, washed with small portions of Et_2O and *n*-pentane, and dried under vacuum (yield 90%). IR (KBr): ν 1617 cm^{-1} (C═N). μ_{eff}: 5.74 μ_B (22 °C). Electronic spectra: (reflectance) 15 650, 14 800, 11 900, 8300, 7050sh, 6000 cm^{-1}. Anal. Calcd (%) for $C_{42}H_{45}Br_2Cl_2CoN_5Ni$ (968.19): C, 52.10; H, 4.68; Co, 6.09; N, 7.23; Ni 6.06. Found: C, 52.01; H, 4.61; Co, 5.99; N, 7.18; Ni 6.00.

Synthesis of $^{Me}N_5NiBr_2$. A solid sample of $NiBr_2 \cdot MeOCH_2CH_2OMe$ (77 mg, 0.248 mmol) was added to a yellow solution of $^{Me}N_5$ (154 mg, 0.248 mmol) in Et_2O (30 mL) under stirring at room temperature. Within a few minutes the solid dissolved, giving an orange solution. After 16 h, the formed orange precipitate was collected by decantation, washed with small portions of Et_2O and *n*-pentane, and dried under vacuum (yield 85%). IR (KBr): ν 1618 cm^{-1} (C═N). μ_{eff}: 2.85 μ_B (22 °C). Electronic spectra: (reflectance) 22 600sh, 12 500, 8100 cm^{-1}; (absorption) 22 600 (ϵ 80), 13 300 (ϵ 24), 8200 (ϵ 28) cm^{-1}. Anal. Calcd (%) for $C_{43}H_{49}Cl_2NiN_5$ (838.35): C, 60.17; H, 5.41; Ni, 7.00; N, 8.35. Found: C, 60.11; H, 5.35; Ni, 6.91; N, 8.24.

Synthesis of $^{iPr}N_6Co_2Cl_4$. A mixture of $CoCl_2$ (13 mg, 0.104 mmol) and $^{iPr}N_6$ (50 mg, 0.052 mmol) in THF (3 mL) was stirred overnight at room temperature. The formed light brown precipitate was filtered on a sintered-glass frit, washed with Et_2O, and dried in a stream of nitrogen (yield 87%). IR (KBr): ν 1594 cm^{-1} (C═N). μ_{eff}: 6.45 μ_B (22 °C). Electronic spectra: (reflectance) 18 200sh, 14 500, 11 100, 8000, 6600 cm^{-1}; (absorption) 18 100sh, 14 200 (ϵ 80), 11 100 (ϵ 10), 8000 (ϵ 28), 6600 (ϵ 28) cm^{-1}. Anal. Calcd (%) for $C_{66}H_{84}Cl_4Co_2N_6$ (1221.11): C, 64.92; H, 6.93; N, 6.88. Found: C, 64.88; H, 6.98; N, 6.90.

Synthesis of $^{iPr}N_6Fe_2Cl_4$. A mixture of $FeCl_2$ (13 mg, 0.104 mmol) and $^{iPr}N_6$ (50 mg, 0.052 mmol) in THF (3 mL) was stirred overnight at room temperature. The formed green precipitate was filtered on a sintered-glass frit, washed with Et_2O, and dried in a stream of nitrogen (yield 85%). IR (KBr): ν 1596 cm^{-1} (C═N). μ_{eff}: 7.27 μ_B (22 °C). Electronic spectra: (reflectance) 13 400, 5200 cm^{-1}; (absorption) 13 200 (ϵ 1000), 5200 (ϵ 24) cm^{-1}. Anal. Calcd (%) for $C_{66}H_{84}Cl_4Fe_2N_6$ (1214.94): C, 64.92; H, 6.93; N, 6.88. Found: C, 64.92; H, 6.91; N, 6.89.

General Procedure for Ethylene Polymerization. A 500 mL stainless steel reactor was heated to 60 °C under vacuum overnight and then cooled to room temperature under a nitrogen atmosphere.

Monometallic Catalyst Precursors. Procedure A. The solid precatalyst (12 μmol) was charged into the reactor, which was sealed and placed under vacuum. A toluene solution of MAO (3600 μmol), prepared by diluting 2.4 mL of a standard solution of MAO (10 wt % in toluene) in 97.6 mL of toluene, was then introduced into the reactor by suction.

Procedure B. A solution (1.2 mL) of MAO in toluene (1800 μmol) was diluted with 96.3 mL of toluene, and the resultant solution was introduced by suction into the reactor previously evacuated by a vacuum pump. The system was pressurized with ethylene to the desired pressure and stirred for 5 min. The ethylene pressure was then released slowly, and 2.5 mL of a precatalyst solution, prepared by dissolving the solid precatalyst (12 μmol) in 50 mL of toluene, was syringed into the reactor.

Procedure C. A solution (2.4 mL) of MAO in toluene (3600 μmol) was diluted with 96.6 mL of toluene, and the resultant solution was introduced by suction into the reactor previously evacuated by a vacuum pump. The system was pressurized with ethylene to the desired pressure and stirred for 5 min. The ethylene pressure was then released slowly, and 1.0 mL of a precatalyst solution, prepared by dissolving the solid precatalyst (12 μmol) in 50 mL of toluene, was syringed into the reactor.

Bimetallic Catalyst Precursors. Procedure A′. The solid precatalyst (6−12 μmol) was charged into the reactor, which was sealed and placed under vacuum. A toluene solution of MAO (3600−7200 μmol), prepared by diluting 2.4−4.8 mL of a standard solution of MAO (10 wt % in toluene) in 97.6−95.2 mL of toluene, was then introduced into the reactor by suction.

Procedure B′. A solution (2.4 mL) of MAO in toluene (3600 μmol) was diluted with 92.6 mL of toluene, and the resultant solution was introduced by suction into the reactor previously evacuated by a vacuum pump. The system was pressurized with ethylene to the desired pressure and stirred for 5 min. The ethylene pressure was then released slowly, and 5 mL of a precatalyst

Table 1. Crystallographic Data for $^{iPr}N_5CoCl_2$ and $^{Me}N_5CoBr_2$

	$^{iPr}N_5CoCl_2$	$^{Me}N_5CoBr_2$
empirical formula	$C_{51}H_{63}Cl_2CoN_5$	$C_{42}H_{45}Br_2CoN_5$
fw	875.89	838.58
temperature [K]	203(2)	213(2)
wavelenght [Å]	0.71073	0.71073
cryst syst, space group	triclinic, $P\bar{1}$	monoclinic, $P2_1/n$
a [Å]	9.8615(9)	8.5871(7)
b [Å]	10.8452(8)	27.3894(14)
c [Å]	25.9804(19)	16.7052(13)
α [deg]	89.473(6)	
β [deg]	87.860(7)	101.091(6)
γ [deg]	78.520(7)	
V [Å^3]	2721.1(4)	3855.6(5)
Z, D_c [g m^{-3}]	2, 1.069	4, 1.445
absorp coeff [mm^{-1}]	0.448	2.554
F(000)	930	1716
cryst size [mm]	0.30 × 0.20 × 0.10	0.20 × 0.15 × 0.10
θ range for data collection [deg]	3.98−25.25	3.83−29.98
limiting indices	$-7 \le h < \le 11$	$-12 < \le h < \le 11$
	$-12 < \le k < \le 13$	$-31 < \le k < \le 30$
	$-27 < \le l < \le 31$	$-21 < \le l < \le 21$
no. of reflns collected/unique	15 510/9088	29 744/8892
GOF on F^2	0.967	1.031
no. of data/restraints/params	9088/0/532	8892/0/463
final R indices [$I > 2\sigma(I)$]	R1 = 0.0905, wR2 = 0.1870	R1 = 0.0853, wR2 = 0.1075
R indices (all data)	R1 = 0.1703, wR2 = 0.2253	R1 = 0.2222, wR2 = 0.1475
largest diff peak and hole [e Å^{-3}]	0.437 and −0.486	0.717 and −0.397

solution, prepared by dissolving the solid precatalyst (6 μmol) in 50 mL of toluene, was syringed into the reactor.

Procedure C′. A solution (1.2 mL) of MAO in toluene (1800 μmol) was diluted with 96.3 mL of toluene, and the resultant solution was introduced by suction into the reactor previously evacuated by a vacuum pump. The system was pressurized with ethylene to the desired pressure and stirred for 5 min. The ethylene pressure was then released slowly, and 2.5 mL of a precatalyst solution, prepared by dissolving the solid precatalyst (6 μmol) in 50 mL of toluene, was syringed into the reactor.

Procedure D′. A solution (2.4 mL) of MAO in toluene (3600 μmol) was diluted with 96.6 mL of toluene, and the resultant solution was introduced by suction into the reactor previously evacuated by a vacuum pump. The system was pressurized with ethylene to the desired pressure and stirred for 5 min. The ethylene pressure was then released slowly, and 1.0 mL of a precatalyst solution, prepared by dissolving the solid precatalyst (6 μmol) in 50 mL of toluene, was syringed into the reactor.

Irrespective of the procedure, the reactor was immediately pressurized with ethylene to the desired pressure (4/5 bar) and stirred at 1500 rpm. Ethylene was continuously fed to maintain the reactor pressure at the desired value. The temperature inside the reactor increased solely from the exothermicity of the reaction and reached a maximum value within a few minutes. After 15 min, the reaction was terminated by cooling the reactor to −20 °C, venting off the volatiles, and introducing 2 mL of acidic MeOH (5% HCl v/v). The solid products were filtered off, washed with cold toluene and MeOH, and dried in a vacuum oven at 50 °C. The filtrates were analyzed by GC and GC/MS for detecting the presence of oligomers.

X-ray Diffraction Data. Crystallographic data of $^{iPr}N_5CoCl_2$ and $^{Me}N_5CoBr_2$ are reported in Table 1. X-ray diffraction intensity data were collected on an Oxford Diffraction CCD diffractometer with graphite-monochromated Mo Kα radiation (λ = 0.71073 Å) using ω-scans. Cell refinement, data reduction, and empirical absorption correction were carried out with the Oxford diffraction software and SADABS.[22] All structure determination calculations were performed with the WINGX package[23] with SIR-97,[24] SHELXL-97,[25] and ORTEP-3 programs.[26] Final refinements based on F^2 were carried out with anisotropic thermal parameters for all non-hydrogen atoms, which were included using a riding model with isotropic U values depending on the U_{eq} of the adjacent carbon atoms.

Scheme 4[a]

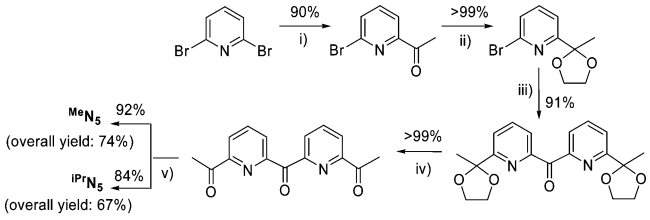

[a] (i) *t*-BuLi, *N*,*N*-dimethylacetamide, Et_2O, -78 °C; (ii) ethylene glycol, *p*-toluenesulfonic acid, benzene, reflux, Dean-Stark apparatus; (iii) *t*-BuLi, methylchloroformate, THF, -78 °C; (iv) HCl 2M, 80-85 °C; (v) aniline, HCOOH, MeOH, reflux.

Results and Discussion

Tris-imino-Bis-pyridine Ligands. The synthetic protocol developed to synthesize the tris-imino-bis-pyridine ligands with either 2,4,6-$Me_3C_6H_2$ (**$^{Me}N_5$**) or 2,6-*i*-$Pr_2C_6H_3$ (**$^{iPr}N_5$**) groups at the imine nitrogen atoms is shown in Scheme 4. 2,6-Dibromopyridine was monolithiated with *t*-BuLi, then treated with *N*,*N*-dimethylacetamide to give 1-(6-bromopyridin-2-yl)ethanone. After the ketone group in the latter compound was protected as *O*,*O*-ketal, the coupling of two pyridine rings was achieved by lithiation of the bromoketal, followed by reaction with methylchloroformate. The deprotection of the carbonyl group under acidic conditions gave the triketone 1-[6-(6-acetylpyridine-2-carbonyl)pyridin-2-yl]ethanone, which was ultimately converted into the desired **N_5** ligand by formic acid-catalyzed condensation with the appropriate aniline in MeOH. Overall yields of 74−67% were consistently obtained.

Tetrakis-imino-Bis-pyridine Ligands. The stepwise procedure developed to synthesize the tetrakis-imino-bis-pyridine

(22) Sheldrick, G. M. *SADABS*, Program for Empirical Absorption Corrections; University of Göttingen: Göttingen, Germany, 1986.
(23) Farrugia, L. J. *J. Appl. Crystallogr.* **1999**, *32*, 837.
(24) Altomare, A.; Burla, M. C.; Cavalli, M.; Cascarano, G. L.; Giacovazzo, C.; Gagliardi, A.; Moliterni, G. G.; Polidori, G.; Spagna, R. *J. Appl. Crystallogr.* **1999**, *32*, 115.
(25) Sheldrick, G. M. *SHELX-97*; Univeristy of Göttingen, 1997.
(26) Burnett, M. N.; Johnson, C. K. *ORTEP-3*, Report ORNL-6895; Oak Ridge National Laboratory: Oak Ridge, TN, 1996.

Scheme 5[a]

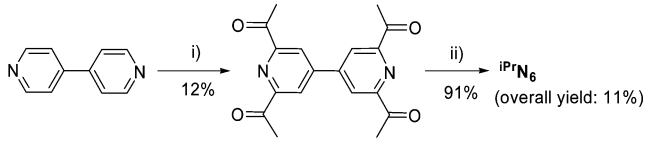

[a] (i) *t*-BuOOH,CH_3CHO; (ii) 2,6-*i*-Pr_2-aniline, HCOOH, *n*-BuOH, reflux.

Scheme 6

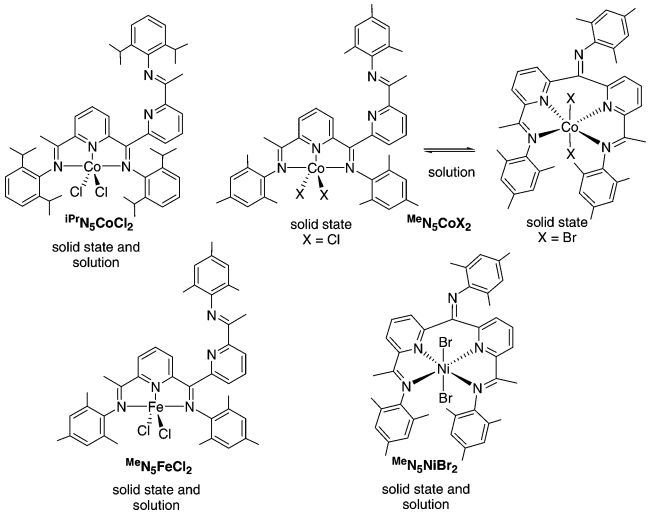

ligand $^{iPr}N_6$ is shown in Scheme 5. The tetra-acetyl-bis(pyridine) intermediate was obtained by a radical reaction involving the treatment of 4,4′-bipyridine with *t*-BuOOH, followed by addition of acetaldehyde.[21] The plain condensation of the resulting tetraketone with 2,6-diisopropylaniline gave the desired $^{iPr}N_6$ ligand. The overall yield was rather low due to the low regioselectivity of the radical reaction.

Monometallic Fe^{II}, Co^{II}, and Ni^{II} Complexes with the $^{iPr}N_5$ and $^{Me}N_5$ Ligands. The monometallic Fe^{II}, Co^{II}, and Ni^{II} complexes with either $^{iPr}N_5$ or $^{Me}N_5$ were isolated as crystalline materials in excellent yields by mixing equimolar amounts of the anhydrous metal dihalides with the appropriate ligand in THF/Et_2O at room temperature. Scheme 6 shows the structures of the isolated complexes as ascertained by single-crystal X-ray analyses or inferred by spectroscopic methods.

All compounds are air-stable in the solid state and in deaerated solutions of polar solvents such as THF, CH_2Cl_2, and 1,2-dichloroethane. In the last solvent they behave as nonelectrolytes. All the complexes have been characterized by elemental analysis, magnetic and spectrophotometric measurements, and IR, ^1H NMR, and X-band EPR spectroscopies. Also, the molecular structures of $^{iPr}N_5CoCl_2$ and $^{Me}N_5CoBr_2$ have been determined by single-crystal X-ray diffraction analyses.

Brown crystals of $^{iPr}N_5CoCl_2$ suitable for an X-ray diffraction study were obtained by recrystallization from warm *n*-butanol. An ORTEP drawing of the molecule contained in the asymmetric unit is shown in Figure 1, while selected bond lengths and angles are reported in Table 2.

The coordination geometry of the cobalt atom can be best described as a distorted square pyramid with the basal plane defined by the N(1), N(2) N(3), and Cl(1) atoms and the Cl(2) atom occupying the apical position.[7a,27] The deviation of the metal center from the coordination plane, defined by N(1), N(2), and N(3), is 0.4803(49) Å, which is comparable to that found for the analogous symmetrical complex $^{iPr}N_3CoCl_2$ ($^{iPr}N_3$ = 2,6-(2,6-*i*-$Pr_2C_6H_3N{=}CMe)_2C_5H_3N$).[7a] The basal halogen atom Cl(1) deviates by 0.1196 (123) Å from the coordination plane

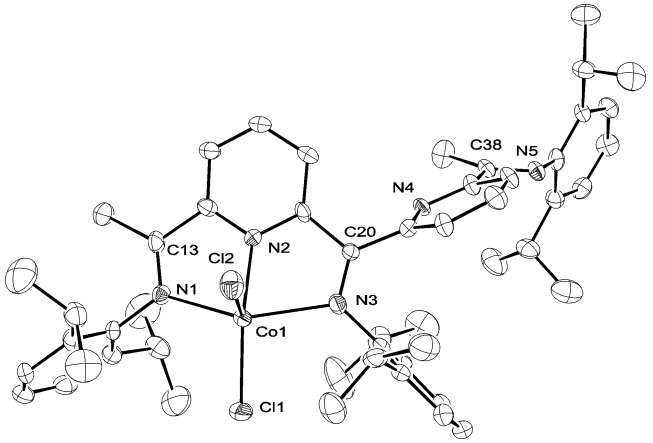

Figure 1. ORTEP drawing of compound $^{iPr}N_5CoCl_2$. Hydrogen atoms are omitted for clarity. Thermal ellipsoids are shown at the 30% probability level.

Table 2. Selected Bond Distances [Å] and Angles [deg] for $^{iPr}N_5CoCl_2$ and $^{Me}N_5CoBr_2$

	$^{iPr}N_5CoCl_2$	$^{Me}N_5CoBr_2$
Co(1)−Cl(1)	2.240(2)	
Co(1)−Cl(2)	2.301(2)	
Co(1)−Br(1)		2.558(1)
Co(1)−Br(2)		2.733(1)
Co(1)−N(1)	2.179(5)	2.146(5)
Co(1)−N(2)	2.045(5)	2.102(5)
Co(1)−N(3)	2.282(5)	2.089(6)
Co(1)−N(4)		2.147(5)
N(1)−C(13)	1.288(8)	
N(1)−C(11)		1.276(8)
N(3)−C(20)	1.290(7)	
N(4)−C(23)		1.288(8)
N(5)−C(38)	1.273(7)	
N(5)−C(17)		1.276(8)
Cl(1)−Co(1)−Cl(2)	118.13(8)	
Br(1)−Co(1)−Br(2)		165.25(4)
N(1)−Co(1)−N(2)	75.1(2)	77.4(2)
N(1)−Co(1)−N(3)	143.6(2)	169.9(2)
N(2)−Co(1)−N(3)	73.5(2)	92.5(2)
N(3)−Co(1)−N(4)		78.0(2)
Intramolecular Short Contact Distances [Å]		
Br(1)···H(13)		2.833
Br(1)···H(10B)		2.880
Br(2)···H(24B)		2.993
C(5)···H(36)		2.367
H(31C)···H(40A)		2.312
H(7B)···H(9C)		2.335

and is typically sandwiched by the two substituted phenyl rings, which are practically orthogonal to the N3 plane (81.08(32)° (plane with C(1) as *ipso* atom) and 85.98(38)° (plane with C(21) as *ipso* atom)). The apical atom Cl(2) shows a deviation from the N3 coordination plane of 2.7257(38) Å, with a Co−Cl(2) bond length of 2.301(2) Å, which is significantly longer than the basal Co−Cl(1) distance.[7a] Due to the asymmetry of the molecule, the Co−N(imine) bonds Co(1)−N(1) and Co(1)−N(3) (2.179(5) and 2.282(5) Å, respectively) are significantly different from each other, while the C−N(imine) bond lengths (N(1)−C(13) and N(3)−C(20) of 1.288(8) and 1.290(7) Å, respectively) are typical for coordinated imine groups and comparable to each other within the standard deviation.[7a,27] The free pyridine ring is coplanar neither with the coordination plane

(27) (a) Kooistra, T. M.; Hekking, K. F. W.; Knijnenburg, Q.; de Bruin, B.; Budzelaar, P. H. M.; de Gelder, R.; Smits, J. M. M.; Gal, A. W. *Eur. J. Inorg. Chem.* **2003**, 648. (b) Bianchini, C.; Mantovani, G.; Meli, A.; Migliacci, F.; Zanobini, F.; Laschi, F.; Sommazzi, A. *Eur. J. Inorg. Chem.* **2003**, 1620. (c) Kleigrewe, N.; Steffen, W.; Blömker, T. G.; Kehr, G.; Fröhlich, R.; Wibbeling, B.; Erker, G.; Wasilke, J. C.; Wu, G.; Bazan, G. C. *J. Am. Chem. Soc.* **2005**, *127*, 13955.

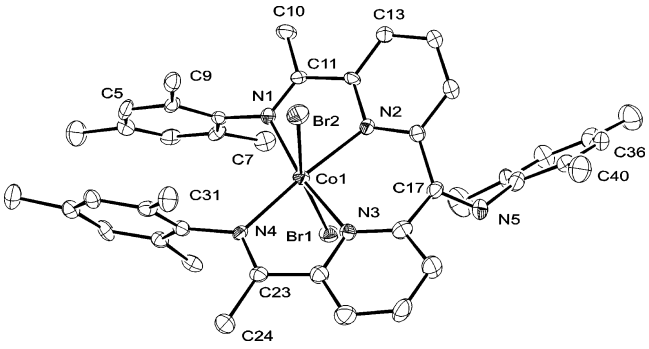

Figure 2. ORTEP drawing of compound $^{Me}N_5CoBr_2$. Hydrogen atoms are omitted for clarity. Thermal ellipsoids are shown at the 30% probability level.

(N1−N3) nor with the uncoordinated imine group, showing dihedral angles of 65.73(0.35)° and 26.85(76)°, respectively.

Consistent with the X-ray crystal structure determination, the IR spectra of $^{iPr}N_5CoCl_2$ are identical both in the solid state and in solution and contain two ν(C═N) bands, one for the coordinated imine groups at 1615 cm^{-1} and one, more intense, for the free imine group at 1648 cm^{-1}, which indicates that not all of the nitrogen atoms of the potentially pentadendate ligand $^{iPr}N_5$ are involved in the coordination to the metal center.[14b,e,28] Details of the IR spectra are reported in the Supporting Information (Figure 1S).

The magnetic and spectrophotometric data of $^{iPr}N_5CoCl_2$, obtained both in the solid state and in solution, are fully consistent with an N_3Cl_2 donor atom set and a coordination geometry closer to a distorted square pyramid than to a trigonal bipyramid.[29,30] The magnetic susceptibility measurements of $^{iPr}N_5CoCl_2$ gave magnetic moments of 4.55 μ_B at room temperature, as expected for a high-spin electronic configuration with three unpaired electrons. The reflectance and absorption vis−NIR spectra (25 000−4550 cm^{-1}) are similar to each other. The absorption spectrum consists of five bands at 6900 (ϵ 25), 8350 (ϵ 15), 11 800 (ϵ 10), 14 600 (ϵ 102), and 17 900sh cm^{-1}, which is in agreement with the spectra of several other five-coordinate Co^{II} (d^7 configuration) complexes with geometry intermediate between C_{4v} and D_{3h}.[29,30] Strong support for a distorted square-pyramidal structure for $^{iPr}N_5CoCl_2$ has been also provided by the solid-state and frozen solution EPR spectra (see below).

Orange crystals of $^{Me}N_5CoBr_2$ suitable for an X-ray diffraction study were obtained by slow diffusion of toluene into a $CHCl_3$ solution of the complex. An ORTEP drawing of the molecule contained in the asymmetric unit is shown in Figure 2, while selected bond lengths and angles are reported in Table 2.

The coordination geometry around the cobalt atom can be described as a distorted octahedron. Four nitrogen atoms, namely, the two imine nitrogen atoms N(1) and N(4) and the two pyridine nitrogen atoms N(2) and N(3), occupy the equatorial positions, while two axially coordinating bromides, with a Br(1)−Co(1)−Br(2) coordination angle of 165.25(4)°, complete the coordination sphere.[31] The metal center deviates from the coordination plane defined by the atoms N(1)−N(4), by 0.0720(31) Å in the direction of Br(1).[31a] Furthermore, the deviation of the four coordinating nitrogen atoms from the latter plane ranges from 0.0530(26) to 0.0626(30) Å. Both pyridine rings are not coplanar, showing a torsion angle of 36.36(1.23)°, which triggers also a deviation of the free imine nitrogen atom (N(5)) from the coordination plane in the direction of Br(1). The apical Co−Br bond lengths are significantly different from each other (2.558(1) and 2.733(1) Å), while the Co−N(imine) distances (2.146(5) and 2.147(5) Å) are significantly longer than the Co−N(pyridine) distances (2.102(5) and 2.089(6) Å). The mesityl groups attached to the N(1) and N(4) atoms are nearly coplanar, showing torsion angles with the best coordination plane of 77.26(21)° (plane with C(25) as *ipso*-atom) and of 72.76(20)° (plane with C(1) as *ipso*-atom). Short intramolecular contacts have been detected in the crystal structure, which might also contribute to build up the overall structural conformation.

Unlike $^{iPr}N_5CoCl_2$, $^{Me}N_5CoBr_2$ is featured by different solid-state and solution IR spectra (see Figure 2S in the Supporting Information). The solution spectrum of $^{Me}N_5CoBr_2$ contains two bands at 1617 and 1642 cm^{-1}, which are characteristic of bonded and free imine groups, respectively, whereas the solid-state spectrum shows only the absorption band at 1617 cm^{-1} due to the coordinated imine.[14b,e,28] This behavior could be indicative either of a change in the cobalt coordination geometry on going from six-coordination (solid state) to five-coordination (solution) or, more likely, of an equilibrium between five- and six-coordinate species. Indirect support for this hypothesis is provided by the intensities of the solution ν(C═N) bands, which are opposite those of the corresponding bands of $^{iPr}N_5CoCl_2$ (see Figure 1S, trace d).

The occurrence of an equilibrium between five- and six-coordinate species in solution is also suggested by the spectrophotometric measurements. Indeed, in agreement with the octahedral geometry adopted in the solid state, the reflectance spectrum of $^{Me}N_5CoBr_2$ shows two spin-allowed transitions at 9900 and 17 800sh cm^{-1}, which are assignable to the $^4T_{1g}(F) \rightarrow {}^4T_{2g}(F)$ and $^4T_{1g}(F) \rightarrow {}^4T_{1g}(P)$ transitions, respectively. Due to the low intensity and vicinity to the highest energy transition, the two-electron transition $^4T_{1g}(F) \rightarrow {}^4A_{2g}(F)$ is not observed.[29a,32a] Unlike the spectrum in the solid state, the absorbance spectrum closely resembles that of the five-coordinate Co^{II} complex $^{iPr}N_5CoCl_2$. However, the spectrum of $^{Me}N_5CoBr_2$ displays also an extra absorption at ca. 10 000 cm^{-1}, which suggests the contemporaneous presence of six-coordinate Co^{II} centers. On the other hand, the presence of two distinct Co^{II} species in solution is also supported by the ^1H NMR and X-band EPR spectra (see below).

On the basis of an in-depth spectroscopic analysis (IR, ^1H NMR, EPR) as well as a comparison with the corresponding characteristics of $^{Me}N_5CoBr_2$ and $^{iPr}N_5CoCl_2$, the complex $^{Me}N_5CoCl_2$ is assigned a five-coordinate structure in the solid state, most likely a distorted trigonal bipyramid, while this complex apparently exists in solution as a mixture of five- and six-coordinate species (see the EPR study reported below).

Like the analogous cobalt derivative, the iron complex $^{Me}N_5FeCl_2$ is featured by a μ_{eff} of 5.36 μ_B at room temperature, consistent with a high-spin electronic configuration. The electronic spectra are very close to those reported for related

(28) Britovsek, G. J. P.; Gibson, V. C.; Spitzmesser, S. K., Tellmann, K. P.; White, A. J. P.; Williams, D. J. *Dalton Trans.* **2002**, 1159.

(29) (a) Sacconi, L.; Morassi, R.; Midollini, S. *J. Chem. Soc. A* **1968**, 1510. (b) Sacconi, L.; Bertini, I.; Morassi, R. *Inorg. Chem.* **1967**, *6*, 1548. (c) Ciampolini, M.; Speroni, G. P. *Inorg. Chem.* **1966**, *5*, 45.

(30) (a) Morassi, R.; Bertini, I.; Sacconi, L. *Coord. Chem. Rev.* **1973**, *11*, 343. (b) Ciampolini, M.; Gelsomini, J. *Inorg. Chem.* **1967**, *6*, 1821.

(31) (a) Hierso, J. C.; Bouwman, E.; Ellis, D. D.; Cabero, M. P.; Reedijk, J.; Spek, A. L. *Dalton Trans.* **2001**, 197. (b) Zangrando, E.; Trani, M.; Strabon, E.; Carfagna, C.; Milani, B.; Mestroni, G. *Eur. J. Inorg. Chem.* **2003**, 2683.

(32) (a) Carlin, R. L. In *Transition Metal Chemistry*; Carlin, R. L., Ed.; Marcel Dekker: New York, 1965; Vol. 1. (b) Sacconi, L. In *Transition Metal Chemistry*; Carlin, R. L., Ed.; Marcel Dekker: New York, 1968; Vol. 4.

Scheme 7

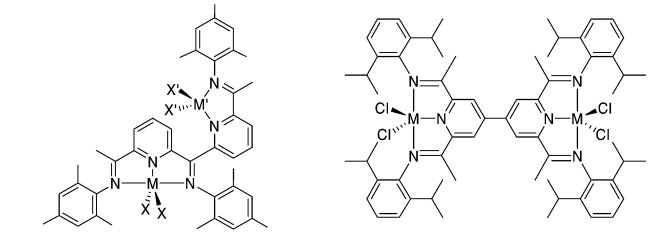

M = Fe, X = Cl; M' = Fe; X' = Cl : $^{Me}N_5Fe_2Cl_4$
M = Co, X = Cl; M' = Fe; X' = Cl : $^{Me}N_5CoFeCl_4$
M = Co, X = Cl; M' = Co; X' = Cl : $^{Me}N_5Co_2Cl_4$
M = Co, X = Br; M' = Co; X' = Br : $^{Me}N_5Co_2Br_4$
M = Co, X = Cl; M' = Ni; X' = Br : $^{Me}N_5CoNiBr_2Cl_2$

M = Fe : $^{iPr}N_6Fe_2Cl_4$
M = Co : $^{iPr}N_6Co_2Cl_4$

five-coordinate bis(imino)pyridine iron complexes.[27b,28−30] In particular, the absorption spectrum displays, in the visible region, a broad and strong absorption (ϵ 1000) at 14 000 cm^{-1}, which is probably due to a ligand-to-metal charge transfer. However, in the NIR region, the spectrum seems to contain also a low-intensity band (ϵ 25) at 4900 cm^{-1}. Generally, high-spin five-coordinate Fe^{II} complexes with an N_3Cl_2 donor atom set show two low-intensity absorption bands, one, in the 10 000−7000 cm^{-1} region, attributed to the spin-allowed d−d transition from the quintet ground state $^5E''$ to the excited state $^5A_1'$ and another below ca. 5000 cm^{-1} for the transition $^5E'' \rightarrow {}^5E'$. It is very likely that the latter transition is responsible for the band observed at 4900 cm^{-1}, whereas the transition $^5E'' \rightarrow {}^5A_1'$ could be masked by the broad absorption centered at 14 000 cm^{-1}, which covers frequencies up to 8000 cm^{-1}. The diffuse reflectance spectrum of solid $^{Me}N_5FeCl_2$ closely resembles that of the complex in solution, thus indicating no significant change in the stereochemistry of the complex on going from solid state to solution. Also, the IR spectra of $^{Me}N_5FeCl_2$ are identical both in the solid state and in solution and contain the two characteristic ν(C═N) bands for coordinated and uncoordinated imine groups at 1617 and 1641 cm^{-1}, respectively. Further information on the five-coordinate solution structure of $^{Me}N_5FeCl_2$ has been obtained by ^1H NMR spectroscopy in CD_2Cl_2 (see below).

Like $^{Me}N_5CoBr_2$ in the solid state, the nickel derivative $^{Me}N_5NiBr_2$ exhibits a six-coordinate metal center, which reflects the tendency of Ni^{II} to form stable 20e^- octahedral complexes. The IR spectra are identical both in the solid state and in solution and exhibit only the absorption band due to the coordinated imine (1618 cm^{-1}). The absorption spectrum shows a band at 8200 (ϵ 28) cm^{-1} and two bands at 13 300 (ϵ 24) and 22 600 (ϵ 80) cm^{-1}. The last band appears as a shoulder over a much stronger absorption band, probably due to charge transfer. These bands are assigned to the transitions from the fundamental state $^3A_{2g}(F)$ to the excited states $^3T_{2g}(F)$, $^3T_{1g}(F)$, and $^3T_{1g}(P)$, respectively.[29a,b,32b] The μ_{eff} of 2.85 μ_B at room temperature falls in the expected range for octahedral nickel(II) complexes.

In the case of the ligand $^{iPr}N_6$, the kinetic preference for bimetallic species even under metal ion deficiency precluded the synthesis of monometallic complexes in analytically pure form (see below).

Homo- and Hetero-bimetallic Complexes with the $^{Me}N_5$ Ligand. The homo- and hetero-bimetallic complexes $^{Me}N_5Fe_2Cl_4$, $^{Me}N_5Co_2Cl_4$, $^{Me}N_5Co_2Br_4$, $^{Me}N_5CoFeCl_4$, and $^{Me}N_5CoNiBr_2Cl_2$ (Scheme 7) were prepared in good yields by mixing equimolecular amounts of the anhydrous metal dihalide (metal = Fe, Co, Ni) in THF with the appropriate monometallic complex in CH_2Cl_2. The homo-bimetallic complexes were alternatively prepared by adding 2 equiv of anhydrous Fe^{II} or Co^{II} dihalide to a solution of the ligand. Crystalline compounds in analytically pure form were obtained from the reaction mixtures on standing overnight. All complexes are relatively air-stable in the solid state. Unlike the monometallic complexes, which are fairly soluble in chlorinated solvents, the bimetallic complexes dissolve only in very polar solvent like DMF, where, however, a color change occurs with formation of other species. For this reason, the bimetallic complexes have been exclusively characterized by solid-state techniques.

The IR spectra of the bimetallic compounds show a ν(C═N) absorption at ca. 1617 cm^{-1}, consistent with the coordination of all nitrogen atoms.

The reflectance spectra of the bimetallic complexes $^{Me}N_5Fe_2Cl_4$ and $^{Me}N_5CoFeCl_4$ show no significant deviations as compared to the mononuclear parents $^{Me}N_5FeCl_2$ and $^{Me}N_5CoCl_2$ due to the fact that tetrahedral FeN_2X_2 chromophores exhibit only one spin-allowed d−d transition detectable only beyond the low-energy limit of our spectrophotometer (4550 cm^{-1}).[33] Unlike $^{Me}N_5Fe_2Cl_4$, the spectra of the bimetallic complexes $^{Me}N_5Co_2X_4$ (X = Cl, Br) are very complex. In particular, absorptions at ca. 8500, 9500, and 17 500 cm^{-1}, assignable to the d−d transitions of CoN_2X_2 chromophores in a tetrahedral environment,[12] are superimposed on the typical bands of high-spin five-coordinate Co^{II} ions.[29] The reflectance spectrum of the hetero-bimetallic complex $^{Me}N_5CoNiBr_2Cl_2$ shows additional bands at 15650 and 6000 cm^{-1}, as compared to the parent cobalt complex, which are ascribed to the presence of a tetrahedral NiN_2X_2 chromophore in the complex molecule.

Like the vis−NIR spectra, the magnetic moments of the bimetallic complexes are indicative of the presence of two high-spin metal centers in either square-pyramidal or tetrahedral geometry. Indeed, the bimetallic complexes exhibit overall μ_{eff} values of 7.04 μ_B (Fe/Fe), 6.42−6.36 μ_B (Co/Co), 6.82 μ_B (Co/Fe), and 5.74 μ_B (Co/Ni), which are in line with the values calculated for metal ion couples of the same type (7.6, 6.7, 7.1, and 6.0 μ_B, respectively).[14e,34]

Bimetallic Fe^{II} and Co^{II} Complexes with the $^{iPr}N_6$ Ligand. As previously anticipated, the formation of bimetallic complexes with the ligand $^{iPr}N_6$ occurs under any ligand/metal ion ratio. The complexes $^{iPr}N_6Fe_2Cl_4$ and $^{iPr}N_6Co_2Cl_4$ were prepared in good yield by mixing 2 equiv of the anhydrous metal dichlorides to the ligand in THF at room temperature. On standing overnight, crystalline solids precipitated in good yield.

The IR spectra of these bimetallic compounds are identical both in the solid state and in solution and show a ν(C═N) absorption at 1594 cm^{-1}, which reflects the coordination of all nitrogen atoms to the metal centers (i.e., see the IR spectrum of $^{iPr}N_3CoCl_2$ reported in Figure 1S, trace b).

The spectrophotometric and magnetic characterization of the bimetallic $^{iPr}N_6$ complexes is unambiguously indicative of the presence of two high-spin metal centers in five-coordinate coordination geometries. In particular, the reflectance and absorption spectra are similar to each other and almost identical to those of the corresponding monometallic complexes with the $^{iPr}N_3$ and $^{iPr}N_5$ ligands. $^{iPr}N_6Fe_2Cl_4$ and $^{iPr}N_6Co_2Cl_4$ exhibit overall μ_{eff} values of 7.27 μ_B and 6.45 μ_B, respectively. These values are comparable to those observed for the bimetallic N_5 complexes, yet they are slightly smaller than those expected for two noninteracting high-spin Fe^{II} or Co^{II} centers (7.6 or 6.7 μ_B).[14e,34]

^1H NMR Characterization of Mono- and Homo-bimetallic Fe^{II} and Co^{II} Complexes. Useful information for assigning the

(33) Cotton, F. A.; Wilkinson, G. *Advanced Inorganic Chemistry*, 4th ed.; John Wiley & Sons: New York, 1980; p 756.
(34) Gerli, A.; Hagen, K. S.; Marzilli, L. G. *Inorg. Chem.* **1991**, *30*, 4673.

Table 3. ^{1}H NMR Assignments for (Imino)pyridine Iron and Cobalt Complexes (CD_2Cl_2, 22 °C, 400.13 MHz)[a]

	$^{Me}N_3CoCl_2$		$^{Me}N_5CoCl_2$ (five-coord species)		$^{Me}N_3FeCl_2$		$^{Me}N_5FeCl_2$	
position	δ	int	δ	int	δ	int	δ	int
Py-H_m	111.02	2	110.81, 108.73 [44.33, 41.76]	1,1,1,1	83.7	2	87.98, 78.91 [9.08, 3.10]	1,1,1,1
Py-H_p	36.28	1	34.12 [4.40]	1,1	40.1	1	40.98 [2.28]	1,1
N=CMe	−0.58	6	−0.33 [3.79]	3,3	−20.5	6	−2.89 [2.05]	3,3
Ar-Me_o	−26.74	12	−26.20, −28.63 [1.17]	6,6,6	12.9	12	12.93 12.23 [1.23]	6,6,6
Ar-H_m	6.40	4	6.58 6.33 [2.94]	2,2,2	15.6	4	17.14 13.94 [6.59]	2,2,2
Ar-Me_p	17.00	6	17.20, 14.57 [2.09]	3,3,3	21.7	6	23.31 21.61 [0.38]	3,3,3

[a] δ between square brackets denotes the uncoordinated (imino)pyridine hydrogens

Table 4. ^{1}H NMR Assignments for (Imino)pyridine Cobalt Complexes (CD_2Cl_2, 22 °C, 400.13 MHz)

	$^{iPr}N_3CoCl_2$		$^{iPr}N_5CoCl_2$	
position	δ	int	δ	int
Py-H_m	116.47	2	122.10 118.05	2,2
Py-H_p	49.39	1	50.01	2
N=CMe	4.36	6	6.50	6
i-Pr-Me	−17.54, −18.74	12,12	−18.7,0−20.27, −20.41, −22.68	12,6,6,12
i-Pr-CH	−84.44	4	−95.20−96.80	4,2
Ar-H_m	10.00	4	9.26−9.39	4,2
Ar-H_p	−8.78	2	−7.49−8.46	1,2

solution structure of some monometallic and bimetallic complexes with the $^{Me}N_5$, $^{iPr}N_5$, and $^{iPr}N_6$ ligands has been obtained by ^{1}H NMR spectroscopy. Unfortunately, the very low solubility of the bimetallic complexes with the N_5 ligands in either hydrocarbon or chlorinated solvents precluded their NMR characterization. The ^{1}H NMR spectra have been acquired in CD_2Cl_2 solutions at 22 °C, and the data obtained are collected in Tables 3, 4, and 5. All protons have been found to resonate at remarkably different chemical shifts as compared to the corresponding protons in the free ligands, which is consistent with the paramagnetic nature of the metal complexes. Consistently, all resonances appear as broad singlets and their assignment has been made on the basis of the relative intensities and line widths (correlated to the proximity to the paramagnetic metal center) as well as by comparison with structurally related paramagnetic Fe^{II} and Co^{II} complexes.[7a,27b,28,35] For comparative purposes, NMR data relative to the 2,6-bis(imino)pyridine complexes $^{iPr}N_3FeCl_2$, $^{Me}N_3FeCl_2$, $^{iPr}N_3CoCl_2$, and $^{Me}N_3CoCl_2$ are reported in the tables ($^{Me}N_3$ = 2,6-(2,4,6-$Me_3C_6H_2N$=CMe)$_2C_5H_3N$).

Overall, the proton chemical shifts of $^{Me}N_5FeCl_2$ follow the trend previously reported for the 2,6-bis(imino)pyridine complex $^{Me}N_3FeCl_2$ (Table 3). In line with the presence of a single, five-coordinate Fe^{II} center, seven proton resonances (δ between square brackets), out of the total 17 signals observed, are easily assigned to the uncoordinated (imino)pyridine portion of the ligand (Figure 3Sa).

Notably, the spectrum of $^{iPr}N_5CoCl_2$ (Figure 3Sb) contains only 14 paramagnetically shifted peaks, instead of the 20 peaks expected for a structure involving a Co^{II} ion bonded to the three nitrogen atoms of the 2,6-bis(imino)pyridine part of the $^{iPr}N_5$ ligand, with the (imino)pyridine moiety free from coordination (Table 4). Consistent with the hindered rotation of the *i*-Pr-substituted aryl rings around the N−C_{aryl} bond, the ^{1}H NMR spectrum of $^{iPr}N_5CoCl_2$ shows four different signals for the CH*Me*$_2$ protons.

Since the IR, vis−NIR, and EPR (see below) characterization of $^{iPr}N_5CoCl_2$ solutions is unambiguously indicative of a Co^{II} center in a distorted square-pyramidal coordination, the ^{1}H NMR spectrum (Figure 3Sb) can be rationalized by assuming the occurrence of a fast rearrangement of the $^{iPr}N_5$ ligand around $CoCl_2$ so as to form a five-coordinate complex using either possible 2,6-bis(imino)pyridine moiety. According to this interpretation, this process would be averaged on the ^{1}H NMR time scale, whereas the other spectroscopic techniques, having faster time scales, would allow one to have a snapshot of the five-coordinate metal center and of the free (imino)pyridyl moiety.

The ^{1}H NMR spectrum of $^{Me}N_5CoCl_2$ is more complex than the previous ones and may be interpreted only by assuming the formation in solution of two equilibrating Co^{II} species, each of which is featured by a specific set of NMR resonances (Table 3). A 17-peak set can be assigned to a five-coordinate species of the type of iron analogue $^{Me}N_5FeCl_2$. These resonances are also similar to those observed for the 2,6-bis(imino)pyridine complex $^{Me}N_3CoCl_2$ (Table 3). A second set of resonances (see Experimental Section) can be tentatively assigned to another species where the Co^{II} center is octahedrally coordinated. This interpretation is consistent with the IR and electronic spectra as well as the frozen solution EPR spectrum at 5 K (see below). It is noteworthy that the ^{1}H NMR spectrum of the bromide derivative $^{Me}N_5CoBr_2$ is practically identical with that of $^{Me}N_5CoCl_2$, except for the low-field shift of all resonances due to replacement of chloride by bromide (see Experimental Section).

The ^{1}H NMR spectra of $^{iPr}N_6Fe_2Cl_4$ and $^{iPr}N_6Co_2Cl_4$ (Table 5) are easily rationalized, as they closely resemble those of the mononuclear 2,6-bis(imino)pyridine analogues, except for the absence of the *p*-hydrogen atoms of the two pyridine rings, which have been sacrificed to couple the two moieties.

EPR Characterization of Mono- and Homo-bimetallic Co^{II} Complexes. In agreement with the fast spin−lattice relaxation time expected for systems containing high-spin Co^{II} centers, all the complexes reported in this paper were EPR-silent at room temperature. The EPR behavior of the Co^{II} complexes was therefore analyzed at very low temperature. The results obtained in the solid state (Figure 3a) and in frozen CH_2Cl_2 solution (Figure 3b) at 4 K are summarized in Table 6. As for the Fe^{II} complexes, their quintuplet ground state and large zero-field splitting (ZFS) make them EPR-silent even at 4 K.

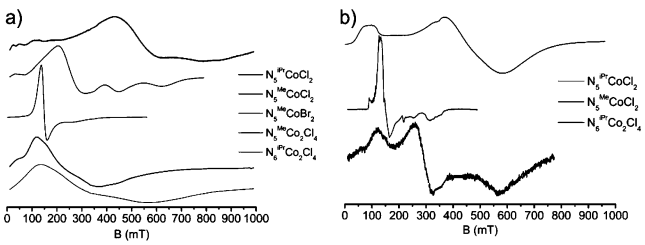

Figure 3. X-Band (9.37 GHz) EPR spectra of Co^{II} complexes at 4 K in the solid-state sample (a) and in frozen CH_2Cl_2 solution (b).

(35) (a) Gibson, V. C.; Long, N. J.; Oxford, P. J.; White, A. J. P.; Williams, D. J. *Organometallics* **2006**, *25*, 1932. (b) Britovsek, G. J. P.; England, J.; Spitzmesser, S. K.; White, A. J. P.; Williams, D. J. *Dalton Trans.* **2005**, 945.

Table 5. ^{1}H NMR Assignments for (Imino)pyridine Iron and Cobalt Complexes (CD_2Cl_2, 22 °C, 400.13 MHz)

	$^{iPr}N_6Fe_2Cl_4$		$^{iPr}N_3FeCl_2$		$^{iPr}N_6Co_2Cl_4$		$^{iPr}N_3CoCl_2$	
position	δ	int	δ	int	δ	int	δ	int
Py-H_m	93.50	4	81.7	2	133.35	4	116.47	2
Py-H_p			81.1	1			49.39	1
N=CMe	−51.98	12	−37.1	6	11.34	12	4.36	6
i-Pr-Me	−4.56, −5.43	24,24	−5.3, −6.3	12,12	−13.45, −16.11	24,24	−17.54, −18.74	12,12
i-Pr-CH	−44.00	8	−22.4	4	−75.78	8	−84.44	4
Ar-H_m	16.40	8	14.9	4	12.57	8	10.00	4
Ar-H_p	−11.55	4	−10.9	2	−7.04	4	−8.78	2

Table 6. Relevant EPR Parameters of Co^{II} Complexes with $^{iPr}N_5$, $^{Me}N_5$, and $^{iPr}N_6$

	solid			CH_2Cl_2 solution		
complex	g_x	g_y	g_z	g_x	g_y	g_z
$^{iPr}N_5CoCl_2$	7.5	1.2	0.9	7.45	1.35	1.35
$^{Me}N_5CoCl_2$	$S = 3/2$ with ZFS			4.4[a]	4.4[a]	2.4[a]
				7.3[b]	3.1[b]	2.1[b]
$^{Me}N_5CoBr_2$	2.4	4.4	4.4			
$^{Me}N_5Co_2Cl_4$	*c*	*c*	*c*	insoluble		
$^{iPr}N_6Co_2Cl_4$	*c*	*c*	*c*	5.4	2.2	1.2

[a] Attributed to six-coordinate species. [b] Attributed to five-coordinate species. [c] Not assignable.

The powder EPR spectrum of $^{iPr}N_5CoCl_2$ shows a typical pattern for an effective $S_{eff} = 1/2$ spin Hamiltonian with a strongly anisotropic *g* factor. Clear evidence of hyperfine structure is observed for the parallel transition, occurring around $g_1 = 7.5$, but not for the partially split perpendicular transition ($g_2 = 1.2$, $g_3 = 0.9$). The observed *g* pattern is consistent with a Co^{II} center in a distorted square-pyramidal geometry,[36] as determined by the X-ray structure analysis (Figure 1). A closely similar pattern is shown by the frozen solution spectrum, with $g_{\|} = 7.45$ and $g_{\perp} = 1.35$, the small differences in the *g* factors being attributable to the different packing effects in the solid state and in the frozen solution. The EPR study therefore confirms that $^{iPr}N_5CoCl_2$ does not change primary structure on going from the solid state to solution.

A different solid-state spectrum is shown by the $^{Me}N_5$ derivative $^{Me}N_5CoCl_2$: the four broad transitions observed can be interpreted only by assuming an $S = 3/2$ system with small ZFS. In such a situation, there are EPR transitions not only within the ground Kramers doublet but also between the two doublets with $M_S = \pm 3/2$ and $M_S = \pm 1/2$. Given that $^{Me}N_5CoCl_2$ is five-coordinate, as indicated by the IR and vis−NIR spectra (*vide infra*), the EPR spectrum suggests a coordination geometry somewhat different from that of $^{iPr}N_5CoCl_2$. A small value of the ZFS can be indicative of a trigonal bipyramidal structure affected by the so-called tetrahedral distortion.[37] It may be useful to recall at this point that the size of the *ortho*-alkyl substituents on the N-aryl rings can control the overall geometry of the $^{R}N_3MCl_2$ complexes (M = Fe, Co; R = *i*-Pr, Me), with the larger *i*-Pr substituents favoring the square-pyramidal coordination and the smaller methyl groups favoring the trigonal-bipramydal geometry.[7a]

Interestingly, on dissolution in CH_2Cl_2, the EPR spectrum of $^{Me}N_5CoCl_2$ changes completely (Figure 3b). Two series of partially hyperfine-split signals are evident with a predominance in intensity of a *g* pattern typical for axially distorted, six-coordinate Co^{II} centers ($g_{\perp} = 4.4$, $g_{\|} = 2.4$).[38] It is worth noticing that a similar pattern is exhibited by the solid-state spectrum of the octahedral $^{Me}N_5CoBr_2$ complex (Figure 3a). One may therefore conclude that also $^{Me}N_5CoCl_2$ can exist as an octahedral complex in solution. On the other hand, the remaining signals in the spectrum of $^{Me}N_5CoCl_2$, at $g_1 = 7.3$, $g_2 = 3.1$, $g_3 = 2.1$, can be safely attributed to a five-coordinate species with a distorted square-pyramidal structure and in lower concentration.

As for the binuclear complexes $^{iPr}N_6Co_2Cl_4$ and $^{Me}N_5Co_2Cl_4$, their EPR spectra in the solid state are characterized by very broad lines that do not allow one to assign the *g* factors to the different transitions (Figure 3a). As for $^{Me}N_5Co_2Cl_4$, the presence of two different chromophores, namely, a Co^{II} ion in a four-coordinate site and a Co^{II} ion in a five-coordinate site, may apparently contribute to originate several unresolved transitions.

A better resolved spectrum was obtained for $^{iPr}N_6Co_2Cl_4$ after dissolution in CH_2Cl_2 solution. The spectrum can be interpreted in terms of an effective $S_{eff} = 1/2$ with a rhombic *g* pattern ($g_1 = 5.4$, $g_2 = 2.2$, $g_3 = 1.2$), while the presence of only one series of signals indicates that the two Co^{II} centers are coordinatively equivalent. A comparison of the solution and solid-state spectra shows that the dissolution of $^{iPr}N_6Co_2Cl_4$ in CH_2Cl_2 has the only effect of sharpening the signals with no major change in the distorted square-pyramidal structure of each metal center.

Polymerization of Ethylene Catalyzed by Mono- and Bimetallic Complexes Stabilized by the N_5 and N_6 Ligands. The mono- and bimetallic complexes with the ligands $^{iPr}N_5$, $^{Me}N_5$ (Table 7), and $^{iPr}N_6$ (Tables 8 and 9) were tested in toluene as catalyst precursors for the polymerization of ethylene under standard experimental conditions.

Upon activation by MAO, the monometallic Fe^{II} and Co^{II} complexes with the $^{iPr}N_5$ and $^{Me}N_5$ ligands formed active catalysts for the polymerization of ethylene, exhibiting comparable activities. Irrespective of the catalyst precursor, high-density polyethylene (HDPE) with no branching was invariably obtained. The weight average molecular weights (M_w) and the polydispersities (M_w/M_n) were typical for this kind of material produced by Fe^{II} and Co^{II} bis(imino)pyridine catalysts.[10]

Irrespective of the metal, the activities of the monometallic N_5 catalysts were significantly higher than those of the corresponding bimetallic derivatives, yet lower than those obtained with the classic $^{R}N_3FeCl_2$ and $^{R}N_3CoCl_2$ precursors under comparable conditions (Table 7). This decrease in productivity may originate for various reasons, for example the capability of the N_5 ligands to wrap the metal center with four nitrogen atoms (Scheme 6), leading to partial formation of catalytically inactive species on treatment with MAO. A role may also be played by the free (imino)pyridine moiety in the five-coordinate complexes that, besides subtracting some activator, may interact with MAO or with the residual $AlMe_3$, leading to less active structures.[39]

(36) Bencini, A.; Gatteschi, D. In *Transition Metal Chemistry*; Figgis, B. N, Melson, G., Eds.; Marcel Dekker: New York, 1982; Vol. 8.

(37) (a) Banci, L.; Bencini, A.; Benelli, C.; Gatteschi, D.; Zanchini, C. *Struct. Bonding* **1982**, *52*, 37. (b) Jiménez, H. R.; Salgado, J.; Moratal, J. M.; Morgenstern-Badarau I. *Inorg. Chem.* **1996**, *35*, 2737.

(38) Abragam, A.; Pryce, M. H. L. *Proc. R. Soc. A* **1951**, *206*, 173.

Table 7. Ethylene Polymerization with Mono- and Bimetallic Precursors of N_5 Ligands[a]

run	precatalyst	M amount (μmol)	MAO amount (μmol)	T_i (°C)	ΔT (°C)	PE amount (g)	TOF[b] ($\times 10^{-5}$)	M_w[c] (kg mol^{-1})	M_w/M_n[c]	T_m[d] (°C)	ΔH[d] (J/g)
1	$^{Me}N_3CoCl_2$	12	3600	27	35	13.5	1.60				
2	$^{iPr}N_5CoCl_2$	12	3600	26	10	5.2	0.61	751	4.1	140.9	139.2
3	$^{Me}N_5CoCl_2$	12	3600	27	27	9.4	1.12	314	14.0	139.1	201.0
4	$^{Me}N_5CoBr_2$	12	3600	22	24	7.2	0.85				
5	$^{Me}N_5Co_2Cl_4$	24	7200	25	19	7.6	0.45	439	14.6	143.0	164.3
6	$^{Me}N_5Co_2Br_4$	24	7200	24	25	8.8	0.52				
7	$^{Me}N_5CoNiCl_2Br_2$	24	7200	27	12	5.7	0.34				
8	$^{Me}N_5CoFeCl_4$	24	7200	26	14	5.3	0.31				
9	$^{Me}N_3FeCl_2$	12	3600	27	45	18.2	2.16				
10	$^{Me}N_5FeCl_2$	12	3600	26	21	9.2	1.09	378	12.0	139.3	199.5
11	$^{Me}N_5Fe_2Cl_4$	24	7200	29	18	10.6	0.63				

[a] Reaction conditions: 500 mL stainless steel reactor; precatalyst, 12 μmol; MAO/M, ratio 300; toluene, 100 mL; ethylene, 4 bar; 15 min, 1500 rpm. [b]TOF expressed as mol C_2H_4 converted (mol metal)$^{-1}$ h^{-1}; average values calculated for 4 runs. [c]Detected by GPC at 140 °C. [d]Detected by DSC.

Table 8. Ethylene Polymerization with $^{iPr}N_6Fe_2Cl_4$ Precursors[a]

run	precatalyst	precatalyst amount (μmol)	Fe amount (μmol)	MAO amount (μmol)	Al/Fe ratio	T_i (°C)	ΔT (°C)	PE amount (g)	TOF[b] ($\times 10^{-5}$)	M_w[c] (kg mol^{-1})	M_w/M_n[c]	T_m[c] (°C)	ΔH[d] (J/g)
1	$^{iPr}N_6Fe_2Cl_4$	6	12	3600	300	23	44	14.2	1.69	413	15.0	139.9	200.5
2	$^{iPr}N_6Fe_2Cl_4$	0.6	1.2	3600	3000	27	37	6.3	7.49				
3	$^{iPr}N_6Fe_2Cl_4$	0.3	0.6	1800	3000	23	7	3.4	8.17				
4	$^{iPr}N_6Fe_2Cl_4$	0.12	0.24	3600	15000	23	8	3.9	22.99				
5	$^{iPr}N_3FeCl_2$	12	12	3600	300	22	51	19.1	2.27				
6	$^{iPr}N_3FeCl_2$	0.6	0.6	1800	3000	22	5	3.3	7.87				
7	$^{iPr}N_3FeCl_2$	0.24	0.24	3600	15 000	22	2	4.0	23.76				

[a] Reaction conditions: 500 mL stainless steel reactor; toluene, 100 mL; ethylene, 5 bar; 15 min; 1500 rpm. [b]TOF expressed as mol C_2H_4 converted (mol metal)$^{-1}$ h^{-1}; average values calculated for 4 runs. [c]Detected by GPC at 140 °C. [d]Detected by DSC.

Table 9. Ethylene Polymerization with $^{iPr}N_6Co_2Cl_4$ Precursors[a]

run	precatalyst	precatalyst amount (μmol)	Co amount (μmol)	MAO amount (μmol)	Al/Fe ratio	T_i (°C)	ΔT (°C)	PE amount (g)	TOF[b] ($\times 10^{-5}$)	M_w[c] (kg mol^{-1})	M_w/M_n[c]	T_m[c] (°C)	ΔH[d] (J/g)
1	$^{iPr}N_6Co_2Cl_4$	6	12	3600	300	26	38	16.1	1.81	485	10.1	142.9	190.5
2	$^{iPr}N_6Co_2Cl_4$	0.6	1.2	3600	3000	25	30	7.1	8.50				
3	$^{iPr}N_3CoCl_2$	12	12	3600	300	24	15	10.4	1.24				
4	$^{iPr}N_3CoCl_2$	1.2	1.2	3600	3000	25	27	4.5	5.35				

[a] Reaction conditions: 500 mL stainless steel reactor; toluene, 100 mL; ethylene, 5 bar; 15 min; 1500 rpm. [b]TOF expressed as mol C_2H_4 converted (mol metal)$^{-1}$ h^{-1}; average values calculated for 4 runs. [c]Detected by GPC at 140 °C. [d]Detected by DSC.

In contrast, the productivity of the Fe^{II} catalyst $^{iPr}N_6Fe_2Cl_4$ was practically identical to that of the congener $^{iPr}N_3FeCl_2$, provided a double proportion of the latter is used (Table 8). Apparently, the coupling of two bis(imino)pyridine moieties via the pyridine C4 carbon atom does not influence the catalytic activity of the Fe^{II} centers.

Unlike $^{iPr}N_6Fe_2Cl_4$, the dicobalt congener $^{iPr}N_6Co_2Cl_4$ was significantly more active than the classic bis(imino)pyridine catalyst $^{iPr}N_3CoCl_2$ (Table 9). This finding is certainly intriguing and worthy of further investigation. At the present stage, we can only emphasize the fact that the two cobalt centers may electronically interact in a conjugated structure such as that of the $^{iPr}N_6$ ligand. In actuality, the electronic delocalization seems to play a significant role in ethylene polymerization by $^{R}N_3CoCl_2$/MAO catalysis. It has been demonstrated by several authors that the action of MAO on the precursors $^{R}N_3CoCl_2$ is quite complex, involving not only the replacement of chloride with methyl and the creation of a coordination vacancy but also, at an initial stage, the formation of diamagnetic square-planar complexes.[40,41] Some authors describe these diamagnetic compounds as containing Co^{I} centers, while other authors propose that the singlet ground state may be due to a square-planar, low-spin Co^{II} center antiferromagnetically coupled to a ligand radical anion; that is, the reduction of high-spin CoX_2L to low-spin CoXL (L = 2,6-bis(imino)pyridine ligand) would occur at the ligand rather than at the metal (Scheme 8).[42] Within this context, yet on a pure speculative basis, the surprisingly high polymerization activity of $^{iPr}N_6Co_2Cl_4$/MAO may be related to the creation of cobalt centers with a favorable electronic structure.

Scheme 8

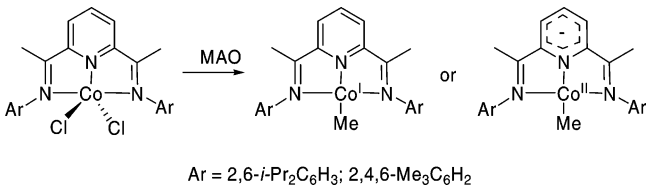

Conclusions

New penta- and hexadentate nitrogen ligands have been synthesized either by coupling 2,6-bis(imino)pyridine and

(39) (a) Knijnenburg, Q.; Smits, J. M. M.; Budzelaar, P. H. M. *Organometallics* **2006**, *25*, 1036. (b) Bruce, M.; Gibson, V. C.; Redshaw, C.; Solan, G. A.; White, A. J. P.; Williams, D. J. *Chem. Commun.* **1998**, 2523.

(40) (a) Humphries, M. J.; Tellmann, K. P.; Gibson, V. C.; White, A. J. P.; Williams, D. J. *Organometallics* **2005**, *24*, 2039. (b) Gibson, V. C.; Humphries, M. J.; Tellmann, K. P.; Wass, D. F.; White, A. J. P.; Williams, D. J. *Chem. Commun.* **2001**, 2252.

(41) Kooistra, T. M.; Knijnenburg, Q.; Smits, J. M. M.; Horton, A. D.; Budzelaar, P. H. M.; Gal, A. W. *Angew. Chem., Int. Ed.* **2001**, *40*, 4719.

(42) Knijnenburg, Q.; Hettershield, D.; Kooistra, T. M.; Budzelaar, P. H. M. *Eur. J. Inorg. Chem.* **2004**, 1204.

(imino)pyridine molecules or by homocoupling 2,6-bis(imino)-pyridine molecules. The presence of five or six nitrogen donor atoms allows these ligands to coordinate either one or two Fe^{II} or Co^{II} bis-halides. In the bimetallic systems with the $\mathbf{N_5}$ ligands, one metal is five-coordinate, generally in a square-pyramidal geometry, and the other is tetrahedrally coordinated. In the monometallic $\mathbf{N_5}$ complexes, depending on the halide (Cl, Br) and on the size of the substituents on the N-aryl rings, either five- or six-coordinate monometallic complexes are formed, which shows that these ligands maintain a high degree of structural flexibility notwithstanding the extensive conjugation provided by uninterrupted sequences of C−C and C−N double bonds.

Effective catalysts for the polymerization of ethylene to HDPE are generated by activating the bis-chloride precursors with MAO in toluene. Of particular relevance is the very good productivity (more than 1.8×10^5 mol C_2H_4 converted (mol cobalt)$^{-1}$ h^{-1}) exhibited by the dicobalt complex $\mathbf{^{iPr}N_6Co_2Cl_4}$, which is more active than any other Co^{II} polymerization catalyst ever reported. The good results obtained in the polymerization of ethylene and the proved, facile structural modification of the (imino)pyridine moiety forecast the use of these $\mathbf{N_5}$ and $\mathbf{N_6}$ ligands in other homogeneously catalyzed reactions.

Acknowledgment. Thanks are due to the European Community (STREP project no. 516972−NANOHYBRID; Network of Excellence no. NMP3-CT-2005-0011730−IDECAT), Ministero dell'Istruzione, dell'Università e della Ricerca (FIRB project no. RBNE03R78E−NANOPACK), and Firenze-HYDROLAB project for financial support. L.S. acknowledges Prof. D. Gatteschi for useful suggestions and the financial support of Ente Cassa di Risparmio di Firenze.

Supporting Information Available: Text and tables giving crystallographic data for compounds $\mathbf{^{iPr}N_5CoCl_2}$ and $\mathbf{^{Me}N_5CoBr_2}$. This material is available free of charge via the Internet at http://pubs.acs.org.

OM7005062